Impact of climate changes on vegetation and human societies during the Holocene in the South Caucasus (Vanevan, Armenia): A multiproxy approach including pollen, NPPs and brGDGTs

Mary Robles, Odile Peyron, Elisabetta Brugiapaglia, Guillemette Ménot, Lucas Dugerdil, Vincent Ollivier, Salomé Ansanay-Alex, Anne-Lise Develle, Petros Tozalakyan, Khachatur Meliksetian, et al.

Impact of climate changes on vegetation and human societies during the Holocene in the South Caucasus (Vanevan, Armenia): a multiproxy approach including pollen, NPPs and brGDGTs

Mary Robles[1,2], Odile Peyron[2], Elisabetta Brugiapaglia[1], Guillemette Ménot[3], Lucas Dugerdil[2,3], Vincent Ollivier[4,5], Salomé Ansanay-Alex[3], Anne-Lise Develle[6], Petros Tozalakyan[7], Khachatur Meliksetian[7], Kristina Sahakyan[7], Lilit Sahakyan[7], Bérengère Perello[8], Ruben Badalyan[9], Claude Colombié[10], Sébastien Joannin[2]

1 - Univ. Molise, Department Agriculture, Environment and Alimentation, Italy
2 - Univ. Montpellier, CNRS, IRD, EPHE, UMR 5554 ISEM, Montpellier, France
3 - Univ. Lyon, ENSL, UCBL, UJM, CNRS, LGL-TPE, F-69007 Lyon, France
4 - Aix-Marseille Univ., CNRS, MCC, UMR 7269 LAMPEA, Aix-en-Provence, France
5 - Aix-Marseille Univ., CNRS, FR ECCOREV, Aix-en-Provence, France
6 - Univ. Savoie Mont Blanc, CNRS, UMR 5204 EDYTEM, Le Bourget-du-Lac, France
7 - National Academy of Sciences of Armenia, Institute of Geological Sciences, Yerevan, Armenia
8 - Univ. Lyon, CNRS, UMR 5133 'Archéorient', Maison de l'Orient et de la Méditerranée, Lyon, France
9 - National Academy of Sciences of Armenia, Institute of Archaeology and Ethnography, Yerevan, Armenia
10 - Univ. Lyon, UCBL, ENSL, UJM, CNRS, LGL-TPE, F-69622, Villeurbanne, France

E-mail: mary.robles@umontpellier.fr

Abstract

Relationships between steppe vegetation, human practices and climate changes in the past are crucial to disentangle human development in Eurasia. In this frame, our study investigates (1) modern pollen-vegetation relationships and (2) changes in vegetation, human activity and climate in the Holocene record of Vanevan peat (south-eastern shore of Lake Sevan, Armenia), using a multiproxy approach including sediment geochemistry (XRF), pollen, Non-Pollen Palynomorphs (NPPs), and branched Glycerol Dialkyl Glycerol Tetraethers (brGDGTs). Climate reconstructions are provided by (1) water-level changes, (2) brGDGTs, and (3) pollen transfer functions (multi-method approach: Modern Analogue Technique, Weighted Averaging Partial Least Squares regression, Random Forest, and Boosted Regression Trees). Modern pollen assemblages are selected along an altitudinal transect in Armenia. They show a dominance of Chenopodiaceae in semi-desert/steppe regions while meadows steppes, subalpine, and alpine meadows are dominated by Poaceae. Past vegetation is characterized by steppes dominated by Poaceae surrounded during the Mid-Holocene (8200-4200 a cal BP) by scarce open woodlands. Humans have influenced the local vegetation, mainly through their agricultural practices present since 5200 a cal BP with several intensification steps. Our reconstruction indicates a climate shift from a cold and arid Early Holocene toward a warmer and more humid Mid-Late Holocene. An aridification trend marks the last 5000 years causing a drop in water level, which allowed humans to live and cultivate on Lake Sevan shores. Arid events are recorded at 6.2 ka, 5.2 ka, 4.2 ka and 2.8 ka a cal BP, which are commonly related to multi-centennial-scale variations of Westerlies activity (North Atlantic Oscillation). Through our temperature reconstruction, we can assign (1) the 5.2 and 2.8 ka events as being cold and probably related to a strong Siberian High, and (2) the 4.2 ka event as being warm associated with high Arabian subtropical pressures in the South Caucasus and the Near East. Our study suggests a significant impact of these arid events on the Lake Sevan shore populations and they are consistent with cultural phases in the South Caucasus, thus showing the impact of climatic variations on cultural, land use and occupation mode development in this crossroad region between Europe, Africa and Asia.

Keywords: Vegetation dynamics; Human impact; Agriculture; Water level changes; Paleoclimate; Arid climate events; Transfer functions; XRF

1. Introduction

Understanding relationships between vegetation, climate, and anthropogenic impact over long time periods is a major goal to stress out human development in arid and steppe environments of Eurasia. Paleoecology is therefore a mandatory approach for the regions characterized by a strong human impact such as the Mediterranean basin or the Near East. The Caucasus is among the areas that have been influenced by humans the longest, since the Neolithic, which witness the rise of agriculture and animal husbandry (ca. around 6000 BC) (Badalyan et al., 2004; Chataigner et al., 2014). The variety of landscapes of the region also resulted from its complex orography, geology, and climate (Volodicheva, 2002). The Caucasus is recognized as a "hotspot" of biodiversity (Connor and Kvavadze, 2008; Solomon et al., 2014) and was an important tree refugium during glacial periods (Connor and Kvavadze, 2008). The current vegetation of the South Caucasus is mainly dominated by steppe or desert (Bohn et al., 2000) and only 8% of Armenia's area is covered by exploited or deteriorated forests (Sayadyan, 2011). In contrast, in the 18th century, the forest covered 18% (Sayadyan, 2011), thus questioning the afforestation rate during the Holocene, either before or after the increasing impact of human societies on the environment and the respective impact of climate and humans on ecosystems.

Paleoecological studies of the South Caucasus have recorded forested phases during the Holocene (e.g. Connor et al., 2018; Messager et al., 2013; 2017). In Armenia however, the vegetation dynamic is more complex and suggests steppes dominance throughout the Holocene (Joannin et al., 2014; Leroyer et al., 2016; Cromartie et al., 2020). At Vanevan, on Lake Sevan's shores, Leroyer et al. (2016) also revealed steppes expansion but, as their core only covers the Mid-Holocene (from 7800 to 5100 a cal BP), this vegetation dynamic cannot be extrapolated for the whole Holocene. Old studies based on palynological records with low temporal resolution have suggested that broadleaf deciduous forests existed around 6000 uncalibrated years on the slopes of Lake Sevan (Takhtajyan, 1941; Tumanyan, 1971; Tumajanov and Tumanyan, 1973; Sayadyan et al., 1977; Sayadyan, 1978, 1983; Moreno-Sanchez and Sayadyan, 2005); archaeological sites have revealed animal remains and statues of animals (deer, bears, wolf and foxes) associated with deciduous forests (Lalayan, 1931; Mnatsakanyan, 1952; Mezhlumyan, 1972) but their chronological frame is not precise enough. Further investigations are required to better understand the history of forest and steppes in the South Caucasus over the Holocene and to connect to nowadays issues with aridification and land use impact on soil erosion.

Several studies suggest that humans have an impact on their environment since the Early Holocene in the Near East, by fostering the maintenance of steppic vegetation with fires (Roberts et al., 2002; Turner et al., 2008, 2010). However, in the South Caucasus the regional fire activities do not increase at this period (Messager et al., 2017; Joannin et al., 2014) and climate seems to play an important role in the delayed regional postglacial reforestation in the Near East and the South Caucasus (Wright et al., 2003; Stevens et al., 2001; Djamali et al., 2010; Leroy et al., 2013; Joannin et al., 2014; Messager et al., 2013, 2017; Leroyer et al., 2016). On the shores of Lake Sevan, humans have a long history and agriculture is attested since 5500 a cal BP (Biscione et al., 2002; Parmegiani and Poscolieri, 2003; Hovsepyan, 2013, 2017). As human activities (e.g. agriculture and deforestation) modify the vegetation structure, composition and diversity, a major challenge is to identify and to distinguish the relationships between climate, human, and vegetation. This issue is particularly difficult to address in places (1) where human neolithization already took place during the Early to Mid-Holocene, (2) where the openness of the landscape is not primarily determined by human pressure, and (3) when the technological advancement (e.g. water management systems, winery and fishery) preserves societies from climate and environmental sudden changes (Lawrence et al., 2016; McGovern et al., 2017; Ollivier et al., 2018; Roberts et al., 2019; Ritchie et al., 2021). Human influence is generally detected in paleoecological records during the Early Bronze Age and becomes obvious during the last 3000 years (e.g. Wick et al., 2003; Cromartie et al., 2020). Moreover, wild cereals and other Poaceae produce pollen grains of *Cerealia*-type pollen, which may have biased the interpretation of anthropogenic pollen occurrence (Van Zeist et al., 1975).

Climate role on vegetation during the Holocene is not very well understood in the Caucasus region because of its complexity, mainly due to seasonality influence and climate mechanisms. Few climate reconstructions based on pollen data are available (Connor and Kvavadze, 2008; Joannin et al., 2014; Leroyer et al., 2016; Cromartie et al., 2020) and the climate of Armenia during the Holocene is poorly documented (Joannin et al., 2014; Cromartie et al., 2020). The abrupt climate changes are difficult to detect and until now the 4.2 ka event, a major climate event around the Mediterranean basin (e.g. Bini et al., 2019), has not yet been detected in the South Caucasus. The climate mechanisms are not totally understood although the role of the North Atlantic Oscillation and the Siberian High is undeniable in this region (e.g. Joannin et al., 2014; Bini et al., 2019). Moreover, human impact can substantially influence pollen-climate relationships even if the impact of this influence on climate reconstructions is often difficult to quantify (Chevalier et al., 2020). Accordingly, pollen-based climate reconstructions from records characterized by a strong human influence need to be evaluated carefully, by comparison with independent climate reconstructions based on other proxies. Molecular biomarkers are an emerging proxy that allow quantitative reconstruction of paleotemperature changes from lake or peat sediments. Specifically, brGDGTs (branched Glycerol Dialkyl Glycerol Tetraethers) or glycerol tetraethers are ubiquitous organic compounds synthesized by bacteria (Weijers et al., 2006; Dearing Crampton-Flood et al., 2020). Although bacteria that produce brGDGTs are still unknown (Sinninghe Damsté et al., 2018), the relationship between brGDGTs assemblages and temperature is well established (Weijers et al., 2004; Schouten et al., 2007) and this new proxy allows annual paleotemperature reconstructions (e.g. Dearing Crampton-Flood et al., 2020; Dugerdil et al., 2021;

Stockhecke et al., 2021). To date, there are very few studies based on comparative approaches including pollen and molecular biomarkers to quantify climate variability over time and more particularly abrupt climate events (Watson et al., 2018; Martin et al., 2020; Dugerdil et al., 2021).

This study aims to document vegetation and climate changes around Lake Sevan in Armenia for the Holocene period. Based on a multi-proxy approach, we provide Holocene high-resolution sediment geochemistry, pollen, Non-Pollen Palynomorphs (NPPs), and molecular biomarkers records from a newly retrieved core in the Vanevan peat, located on the south-eastern shore of Lake Sevan. Our study goals are to:

1) based on a collection of new modern samples from Armenia, understand the modern relationships between pollen and vegetation and reinforce the reliability of pollen-based climate reconstructions by the addition of new samples.
2) reconstruct the Holocene wetland dynamics and water level changes based on XRF data, aquatic pollen taxa and NPPs.
3) reconstruct the Holocene vegetation dynamics and identify the existence of deciduous forests or the persistence of steppes on the slopes of Lake Sevan.
4) identify human activity traces on vegetation records by distinguishing the "agricultural" practices present on the south-eastern shore of Lake Sevan.
5) provide a reliable climate reconstruction for the South Caucasus based on a multi-proxy approach including both brGDGTs and pollen (multi-method approach: MAT (Modern Analogue Technique), WAPLS (Weighted Averaging Partial Least Squares regression), RF (Random Forest) and BRT (Boosted Regression Forest)).
6) finally infer relationships between vegetation dynamics, climate changes, and human practices at a local scale and discuss these results at a regional scale (South Caucasus and Near East).

2. Study site

2.1 Geological and geographical setting

The Caucasus Mountains are situated at the eastern edge of the Near East, between the Black Sea and the Caspian Sea (Fig. 1A). They were formed by the Alpine and Himalayan orogeny with the collision between the Arabian and Eurasian plates (Volodicheva, 2002). Located in the Lesser Caucasus (i.e. a geological structure of the South Caucasus), Lake Sevan has a volcano-tectonic origin. Its northeastern shore is characterized by an ophiolitic structure dating from the Middle Jurassic to Early Cretaceous while the western and southern shores are defined by volcanic ridges dating from the Quaternary (Karakhanian et al., 2000; Sosson, et al., 2010). The lava flows from Porak volcano, located in the southeast, spread towards Lake Sevan and Vanevan peat (40°12'8.83"N, 45°40'24.03"E, Fig. 1AB). Several lava flows may date from the Holocene (Karakhanian et al., 2002). The most important fault system in Armenia, the Pambak-Sevan-Syunik fault system extends through the Porak volcano and

Lake Sevan. Seven strong earthquakes on this fault are attested during the Holocene (Karakhanian et al., 2017).

The hydrological system of Lake Sevan has a negative water balance and a slow turnover (50 years) due to higher evaporation (800 mm/year) than precipitation (360 mm/year) (Leroyer et al., 2016). During the Soviet period, its water was intensively used for irrigation and electricity (Jenderedjian, 2005). Consequently, its level dropped approximately 20 m and its volume decreased by more than 40%. The lake passed from oligotrophic to eutrophic conditions, accompanied by changes in the flora and fauna (Lind and Taslakyan, 2005). Among the 28 rivers draining the lake catchment (3650 km²), the Masrik River is located in the South-East. Prior to the lake lowering and field management during the Soviet time, it crossed a wetland area named Gilli (Jenderedjian, 2005). After the drying of the wetland, the area was used for agricultural (mainly wheat and barley), pastoralism (sheep and cattle), and peat exploitation for fuel.

2.2 Modern climate and vegetation

The climate of Armenia is dominated in winter by dry and cold air masses from Siberian High. However, when these masses are weak, they are replaced by the Westerlies (associated with North Atlantic Oscillation, NAO) with snowfall in winter and rainfall in spring. In summer, the climate is warm and dry, and it is linked to Arabian subtropical high pressure in the west and Asian depression in the east (Volodicheva, 2002; Joannin et al., 2014). In the north of Lake Sevan, the annual precipitation is about 500 mm and the annual temperature is 3°C, with a minimum in January of -8°C and a maximum in August of 15°C (Sevan City meteorological station). The coastal belt of the lake receives between 350 and 450 mm of annual precipitation while the mountain zones receive around 800 mm (Baghdasaryan, 1958). Thunderstorms are common around the lake in late spring, particularly in May-June.

The Armenian vegetation is dominated by steppes and only 8% are represented by forests (Sayadyan, 2011). Armenia has a rich biodiversity and a high level of endemism (Fayvush et al., 2013). The mountainous relief favors very different ecological environments (Stanyukovich, 1973; Volodicheva, 2002; Fayvush et al., 2017). The lower landscapes (480–1200 m a.s.l.) are covered by semi-desert vegetation, dominated by *Artemisia fragrans*. The middle mountains (1200-1800 m a.s.l.) are covered by steppes, mainly dominated by *Stipa* spp., or sparse arid woodland composed by *Pistacia atlantica* subsp. *mutica, Amygdalus fenzliana* and *Rhamnus pallasii.* On the slopes (1700-2300 m a.s.l.) arid woodland may develop with *Juniperus* spp. The upper mountains (1900-2300 m a.s.l.) are characterized by meadow steppe, rich in Poaceae. The subalpine mountains (2300-2900 m a.s.l.) are covered by subalpine meadows, generally dominated by *Festuca varia*, and some *Quercus macranthera* woodlands. The alpine mountains (2700-3700 m a.s.l.) are covered by alpine meadows rich in Poaceae (such as *Poa alpina*) and including *Taraxacum stevenii*, *Alchemilla* spp*., Potentilla* spp*., Primula* spp., *Geranium* spp., *Campanula* spp. and *Pedicularis* spp. The vegetation around Lake Sevan is mostly composed of meadow steppes dominated by Poaceae. Only the borders of the lake have trees, principally pines planted during the 1980s and some arid woodland on north-facing slopes. In the southeast slopes of Lake Sevan, some *Juniperus* spp. are also present. The detailed description of potential vegetation of Bohn et al. (2000) around Lake Sevan is presented in Leroyer et al. (2016). At a local scale, the vegetation of Vanevan peat is dominated by Poaceae, Cyperaceae and Juncaceae.

2.3 Archeology and modern human activities

During the Holocene, the first signs of human occupation (hunter-gatherers) in Armenia have been recorded during the Mesolithic in the lower Kasakh valley (Arimura et al., 2012). Agriculture is established during the Late Neolithic (8000-7500 a cal BP) on the Ararat plain (Badalyan et al., 2004; Hovsepyan and Willcox, 2008; Badalyan and Harutyunyan, 2014) where cereals, vetch and lentil have all been recorded along with the presence of sheep (*Ovis aries*), goat (*Capra hircus*), cattle (*Bos taurus*) and scant evidence of pigs (*Sus domesticus*) (Hovsepyan and Willcox, 2008). On the shore of Lake Sevan, the first traces of agriculture date around 5500 a cal BP during the Early Bronze Age (Hovsepyan, 2013, 2017). During the Early, Mid-, and Late Bronze Ages, Early Iron Age, and medieval period, cereals are the primary subsistence crop in the southeast of Lake Sevan around Gilli wetland (Biscione et al., 2002; Parmegiani and Poscolieri, 2003; Hovsepyan, 2013, 2017). The long-term occupation of this area is also attested by the presence of many tombs in Gilli wetland (Fig. 1C). Several empires including the Persians (Achaemenids and Sassanids), Arabs, and Mongols and states including Urartu, Ottoman Turkey, Imperial Russia, and the USSR have succeeded in Armenia (Lindsay and Smith, 2006). The Urartian Empire was present during the Iron Age and centered around Lake Sevan (Biscione et al., 2002; Parmegiani and Poscolieri, 2003). During this period subsistence focused on the cultivation of cereals, vines, fruit trees, and pastoralism. Today, the activities are centered around agriculture and extensive pastoralism. To date, no pollen study has been able to compare pollen indicators of human activities with archeological findings in the Sevan area. In the work done by Leroyer et al. (2016) at Vanevan, the pollen sequence does not cover the last 5700 years BP.

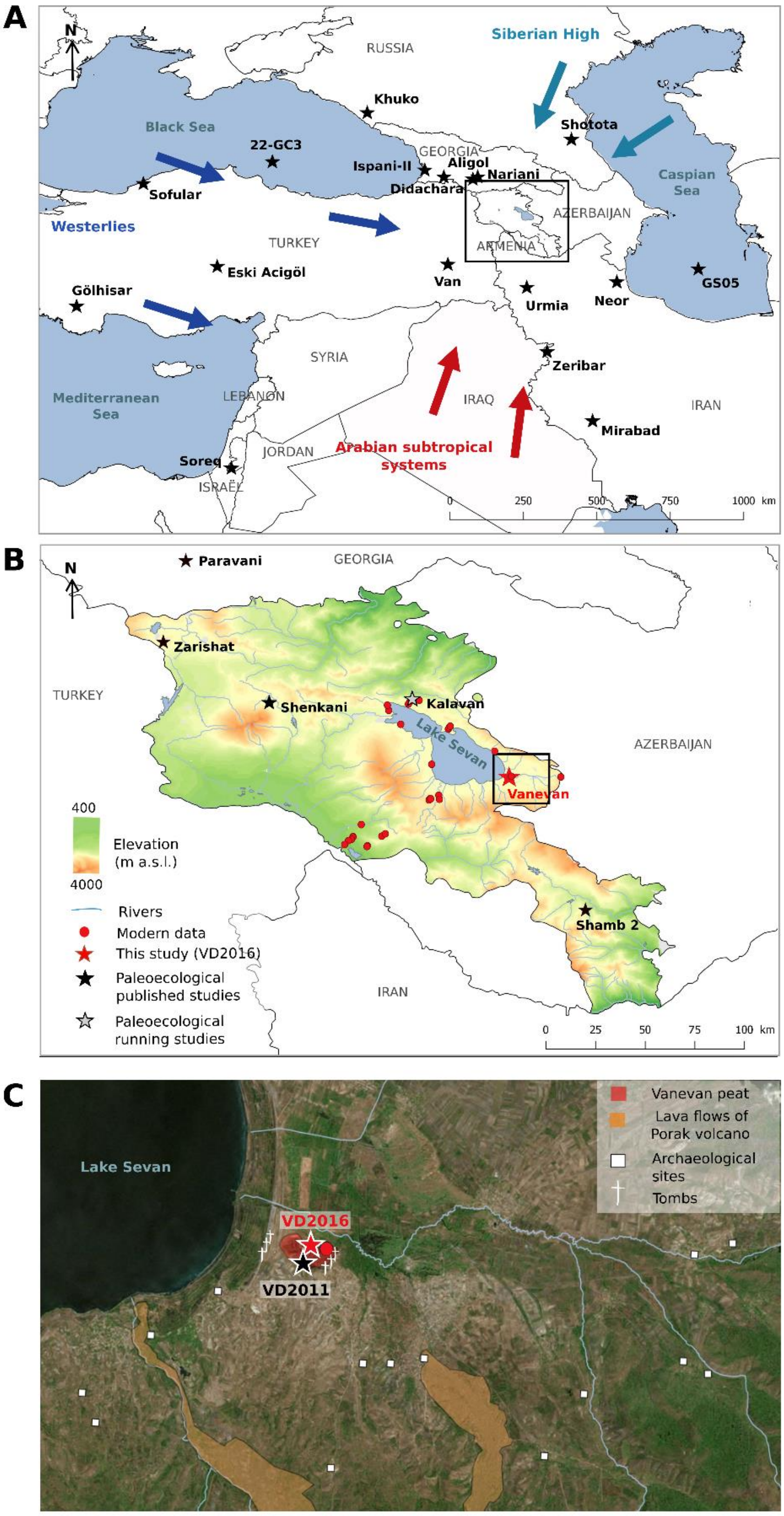

Figure 1. A) East Mediterranean region with selected paleoenvironmental studies: Lake Khuko (Grachev et al., 2020), Shotota swamp (Ryabogina et al., 2018), 22-GC3 (Shumilovskikh et al., 2012), Ispani-II mire (Connor and Kvavadze, 2008), Lake Aligol (Connor and Kvavadze, 2008), Didachara Mire (Connor et al., 2018), Nariani wetland (Messager et al., 2017), Sofular cave (Göktürk et al., 2011), Lake Van (Wick et al., 2003), Eski Acigöl (Roberts et al., 2001), Lake Neor (Sharifi et al., 2015), Lake Urmia (Djamali et al., 2008), Lake Gölhisar (Eastwood et al., 2007), GS05 (Leroy et al., 2013), Lake Zeribar (Stevens et al., 2001), Lake Mirabad (Stevens et al., 2006), Soreq cave (Bar-Matthews et al., 1997). B) Topography of Armenia with the location of Vanevan peat and modern samples (mosses, soils and botanical records). Black and gray stars represent published and ongoing

paleoecological studies, respectively: Lake Paravani (Messager et al., 2013; 2073 m), Zarishat fen (Joannin et al., 2014; 2116 m), Lake Shenkani (Cromartie et al., 2020; 2193 m), Lake Kalavan (Joannin et al., in prep; 1603 m), Shamb 2 (Ollivier et al., 2011). C) Southeastern shore of Lake Sevan with the location of Vanevan peat (VD2016 core, this study; VD2011 core, Leroyer et al., 2016) and archeological sites (Biscione et al., 2002; Parmegiani and Poscolieri, 2003; Hovsepyan, 2013, 2017). Image modified from Google Earth (Image © 2020 CNES/Airbus, © 2019 Google, © 2019 Basarsoft).

3. Material and methods

3.1 Field campaign

3.1.1 Core retrieval

The present study focuses on a new core VD2016 (40°12’8.83”N, 45°40’24.03”E, 1916 m a.s.l.) retrieved from approximately 850 meters north of the previous Vanevan study (Fig. 1C). Two parallel cores (cores A and B) were taken with a 1 m Russian corer with a 6.3 cm diameter chamber. The mastercore (MC), was built from sections of both cores using the lithology and XRF data for correlation. The complete continuous sequence measures 601 cm in total.

3.1.2 Modern samples

A total of 28 modern pollen samples along an altitudinal transect from the Ararat plain (808 m a.s.l.) to the mountains of Lake Sevan (2699 m a.s.l.) were collected in May 2016, 2017, and 2019 (Fig. 1B and Supplementary Table S1). This transect records the vegetation in semi-desert steppes, meadow steppes, subalpine, and alpine meadows in Armenia (Stanyukovitch, 1973; Volodicheva, 2002). Several sampling sites are located around Lake Sevan and three altitudinal transects were performed in the mountains around it (Mount Artanish, Mount Armaghan, and Mount Katarajayr). In each sampling site, 2-5 moss polsters or soil were collected within a radius of 5 m and then combined into one sample. The vegetation within a radius of 10 m, representing the local vegetation, was recorded by visual estimation of percentage cover for 19 sites (adaptation of the Braun-Blanquet method; Braun-Blanquet and Schoenichen, 1964). For the other sites, the local vegetation was not quantitatively identified but qualitatively estimated. The vegetation within a radius of 100 m is considered as the extra-local vegetation and beyond this distance as the regional vegetation. The modern climate data were calculated with the *New_LocClim 1.10* software (Grieser et al., 2006) and then corrected according to the site elevation.

3.2 Age model, lithology, and geochemistry

3.2.1 Age model and lithology

The core chronology is based on 12 accelerator mass spectrometry (AMS) ^{14}C dates (Table 1). For seven samples, plant macrofossils (plant fibers, seeds) and charcoal were selected for dating. In addition, bulk sediment was used for another set of 5 samples in which the quantity of macrofossils was insufficient. Radiocarbon ages were calibrated in years cal BP using *Calib 8.2* software with the

IntCal20 calibration curve (Reimer et al., 2020) and the median calibrated ages with the 2 σ confidence intervals (95%) are reported in Table 1. The age-depth model was constructed using an interpolated linear curve with the R 'Clam' program with 95% confidence intervals (Blaauw, 2010). Three zones were defined upon visual differences in lithology.

Table 1. AMS-radiocarbon dates (Radiocarbon Laboratory, Poznań), calibrated median ages, with 2 σ range of calibration from Vanevan peat A and B cores. *: Age rejected

Sample ID	Depth MC (cm)	Lab code	Material	AMS 14C age (a BP)	Age (a cal BP) (2 σ)	Median age (a cal BP)
A0 15-17	15	Poz-111218	Plant fibers	875 ± 30	692-903	768
A0 42-43	42	Poz-88797	Plant fibers	1860 ± 50	1623-1916	1773
A1 16-17	59	Poz-110035	Plant fibers, seeds	2355 ± 35	2326-2665	2377
A1 55-57	98	Poz-89222	Plant fibers	4380 ± 40	4848-5255	4943
A2 16-17	126	Poz-110036	Plant fibers, seeds	4400 ± 35	4859-5263	4966
A2 56-57	165	Poz-119280	Plant fibers, charcoals, seeds	4450 ± 30	4885-5284	5112
A2 86-87*	195	Poz-122005	Bulk	6605 ± 35	7429-7568	7495
A3 39-40	247	Poz-122006	Bulk	6690 ± 35	7479-7651	7554
A3 81-82	289	Poz-119285	Bulk	6920 ± 40	7670-7842	7746
A5 80-81	486	Poz-119281	Bulk	7980 ± 50	8646-8998	8844
B5 29-31	534	Poz-89221	Plant fibers	8230 ± 40	9026-9401	9197
A6 91-92*	597	Poz-121074	Bulk	6980 ± 50	7690-7931	7810

3.2.2 Geochemistry

The running chemical composition of the sediment cores was performed using an Avaatech XRF (EDYTEM Laboratory) core scanner at a 0.5 cm interval (elements presented here: Si, K, Ti, Al, S, Fe, Ca, Mg, P). XRF measurements were carried out on split cores with a duration step of 10 s. A 10 kV voltage and a 1000 µA current was applied to detect elements. Because of the influences of variable water content and grain size on the sediment matrix, the XRF scanner provides an estimate of the geochemical composition, and the acquired counts are semi-quantitative. The selected elements are indicative of the sediment geochemistry itself depending on erosive and deposit conditions, and of sources in the catchment (Croudace and Rothwell, 2015). Principal component analysis (PCA) was performed on XRF data with *FactoMineR 2.4* package (Lê et al., 2008). Titanium (Ti) content is considered as a terrigenous indicator because it is weakly affected by weathering and redox conditions (Arnaud et al., 2012). Silicon (Si) content may be derived from diatoms, radiolaria, siliceous sponges, or from phytoliths contained in aquatic and terrestrial plants. The ratio Si/Ti allows to understand the respective role of organic production or terrigenous inputs (Brown et al., 2007).

3.3 Pollen, NPP analysis, and pollen-inferred climate reconstruction

3.3.1 Pollen, NPP extraction, and counting

A total of 28 modern and 94 fossil pollen samples from the Vanevan core (2 cm resolution between 43-99 cm, 4 cm resolution between 99-170 cm, 10 cm resolution between 170-600 cm) were extracted for analysis. For each sample, 1 cm^3 of sediment was processed and 3 *Lycopodium* tablets were added to calculate the absolute abundance of pollen grains. The core samples were treated with the standard procedure (Fægri et al., 1989; Moore et al., 1991) including HCl, KOH, acetolysis and HF. The pollen and NPP counts were carried out with a Leica DM1000 LED microscope at a standard magnification of 400x. Pollen and NPP taxa were identified using photo atlases (Reille, 1992–1998; Komárek and Jankovská, 2001; Van Geel, 2002; Beug, 2004) and a modern reference collection (ISEM, University of Montpellier). A minimum of 300 or 200 pollen grains of terrestrial taxa (excluding aquatic plants, mainly Cyperaceae) was counted by slide for the richest and the poorest samples, respectively, to obtain a representative assessment of pollen types (Lytle and Wahl, 2005; Djamali and Cilleros, 2020). Grass pollen grains greater than 40 µm were classified as *Cerealia*-type (Beug, 2004). Aquatic taxa, fern spores, and NPPs (algae and fungal spores) were counted alongside pollen. The pollen diagrams were constructed with the R package *Rioja* (Juggins, 2020).

3.3.2 Pollen-inferred climate reconstruction

To reconstruct climate parameters from pollen data, currently available methods have their own set of advantages and limitations and the selection of the most appropriate technique to be used on the fossil pollen record can be complex. A multi-method approach is the best choice to increase the reliability of the climate reconstruction (e.g. Brewer et al., 2008; Peyron et al., 2013; Salonen et al., 2019). Four methods have been selected here among the most accurate (Chevalier et al., 2020): the Modern Analog Technique (MAT; Guiot, 1990), Weighted Averaging Partial Least Squares regression (WAPLS; Ter Braak and Van Dam, 1989; Ter Braak et al., 1993), and regression Trees: Random Forest (RF; Breiman, 2001; Prasad et al., 2006) and Boosted Regression Trees (BRT; De'ath, 2007; Elith et al., 2008). The MAT and the WAPLS are often selected to reconstruct past climate changes while RF and BRT have been developed recently to reconstruct palaeoclimate changes (Salonen et al., 2016, 2019) and have never been tested on Caucasus pollen records. Based on machine learning, these classification trees are used to partition the data by separating the pollen assemblages based on the relative pollen percentages. RF is based on a large number of regression trees, each tree being estimated from a randomized ensemble of different subsets of the modern pollen dataset by bootstrapping. BRT is also based on regression trees and differs from RF in the definition of the random modern datasets. In RF, each sample gets the same probability of being selected, while in BRT the samples that were insufficiently described in the previous tree get a higher probability of being selected. This approach is called ‘boosting’ and increases the performance of the model over the elements that are least well predicted.

The modern pollen dataset used here (382 samples) is part of the large Eurasian/Mediterranean dataset compiled by Peyron et al., (2013, 2017) which include more than 3200 modern pollen samples (moss polster, soils and top-cores). A recent study showed that (1) large databases are not reliable for the reconstruction of steppic environment/climate and (2) local calibrations including data from steppe and desert–steppe sites are necessary to better calibrate arid environments (Dugerdil et al., 2021). Therefore, the large database has been cropped to optimize the selection of surface samples consistent with our paleosequence environment: we used here a reduced dataset of 382 "cold steppe" samples, including new samples from Mongolia (Peyron et al., 2013, 2017; Dugerdil et al., 2021), Georgia (Connor et al., 2004) and Armenia (seventy-five new modern samples, this study). We applied here a biome constraint (Guiot et al., 1993), which is essential to define steppe environments and to distinguish between cold and warm steppes. Therefore, we have finally used for the calibration of each method the samples attributed to the biomes "cold steppes" following the biomization procedure (Prentice et al., 1996; Peyron et al., 1998). The location of these 382 cold steppe samples is given in the Supplementary Fig. S2. The surface calibration methods and datasets to reconstruct paleoclimate in arid environments are discussed in Dugerdil et al., (2021). In order to estimate the performance of each method, the transfer functions have been tested on the modern "cold steppe" dataset, 60% of the dataset has been used to calibrate and 40% to test the transfer functions, thereby preventing a circular reasoning. Correlations have been realized between the current climate parameters extracted from WorldClim 2 (Fick and Hijmans, 2017) and the estimated climate parameters reconstructed by each method (Supplementary Fig. S3). Then, the performance of each method and each calibration training was statistically tested with a bootstrap technique (for more details, see Dugerdil et al., 2021). The transfer functions have been applied 500 times on the modern "cold steppe" dataset, thereby obtaining the Root Mean Square Error (RMSE) and the R^2 and determining if modern samples are suitable for quantitative climate reconstructions (Supplementary Table S4). Thereafter, the function transfers have been applied on the Vanevan core samples with the modern "cold steppe" dataset. Four climate parameters were reconstructed, mean annual air temperature (MAAT), mean annual precipitation (MAP), mean temperature of the warmest month (MTWA), and summer precipitation (Psummer) including July, August, and September. For each climate parameter, the methods fitting with the higher R^2 and the lower RMSE were selected. The WAPLS and the MAT methods were applied with the R package Rioja (Juggins, 2020), the RF with the R package randomForest (Liaw and Wiener, 2002) and the BRT with the R package dismo (Hijmans et al., 2020). Cyperaceae and ferns of Vanevan record have been excluded because they indicate local dynamics in Armenia (Joannin et al., 2014; Cromartie et al., 2020).

3.4 GDGT analysis and annual temperature reconstruction

3.4.1 BrGDGT analyses

A total of 46 core samples (4-20 cm resolution) were used for GDGT analysis. After freeze-drying and grounding, a subsample (0.8 g for soil, 1 g for clay and 0.6 g for peat sediments) was extracted using a Microwave oven (MARS 6; CEM) with a mix of dichloromethane and methanol (3:1). The total lipid extract was split on a silica SPE cartridge, using hexane: DCM (1:1) and DCM:MeOH (1:1). GDGTs were analyzed using a High-Performance Liquid Chromatography Mass Spectrometry (HPLC-APCI-MS, Agilent 1200) with detection via selective ion monitoring (SIM) of m/z 1050, 1048, 1046, 1036, 1034, 1032, 1022, 1020, and 1018 for brGDGTs (Hopmans et al., 2016; Davtian et al., 2018). GDGT concentrations were calculated based on the internal standard (C_{46} GDGT, Huguet et al., 2006). The linearity and analytic reproducibility were assessed based on an internal standard sediment.

3.4.2 brGDGT-based proxy calculation and global calibration datasets

The formulae for the brGDGT indexes are presented in Table 2. The proportions of tetra- (I), penta- (II) and hexa- (III) methylated brGDGTs were calculated with the fractional abundances of brGDGTs including the 5-methyl (X), the 6-methyl (X') and the 7-methyl brGDGT (X_7) (Ding et al., 2016). The ΣIIIa/ΣIIa ratio proposed by Xiao et al. (2016) was calculated according to the equation modified by Martin et al. (2019) including the 5-, 6- and 7-methyl brGDGTs. The CBT and MBT indexes were developed by Weijers et al. (2007) and the MBT'_{5me}, only based on the 5-methyl brGDGTs, by De Jonge et al. (2014). The mean annual temperature was calculated with the global soil calibration developed by Naafs et al. (2017a) and the global lacustrine calibration developed by Sun et al. (2011). The calibrations are applied according to the sediment types in paleorecords (e.g. Martin et al., 2019) and can be homogenized using a ΔMAAT based on the mean value of each sediment type. The analytic reproducibility corresponds to 0.005 for CBT, 0.006 for MBT, 0.008 for MBT'_{5me}, 0.3 for $MAAT_{soil5me}$ and 0.2 for $MAAT_{lake}$.

Table 2. Synthesis of the formulae for the main brGDGT indices

Indice	Formula	Reference
$\%tetra$	$\frac{Ia + Ib + Ic}{\Sigma brGDGTs}$	Ding et al., 2016
$\%penta$	$\frac{IIa + IIa' + IIa_7 + IIb + IIb' + IIb_7 + IIc + IIc' + IIc_7}{\Sigma brGDGTs}$	Ding et al., 2016
$\%hexa$	$\frac{IIIa + IIIa' + IIIa_7 + IIIb + IIIb' + IIIb_7 + IIIc + IIIc' + IIIc_7}{\Sigma brGDGTs}$	Ding et al., 2016
$\Sigma\, IIIa/\Sigma\, IIa$	$\frac{IIIa + IIIa' + IIIa_7}{IIa + IIa' + IIa_7}$	Martin et al., 2019
CBT	$-log\frac{Ib + IIb}{Ia + IIa}$	Weijers et al., 2007

MBT	$\frac{Ia + Ib + Ic}{\Sigma brGDGTs}$	Weijers et al., 2007
MBT'_{5me}	$\frac{Ia + Ib + Ic}{Ia + Ib + Ic + IIa + IIb + IIc + IIIa}$	De Jonge et al., 2014
$MAAT_{soil5me}(°C)$	$39.09 \times MBT'_{5me} - 14.50 (n = 177, R^2 = 0.76, RMSE = 4.1°C)$	Naafs et al., 2017a
$MAAT_{lake}(°C)$	$3.949 - 5.593 \times CBT + 38.213 \times MBT (n = 100, R^2 = 0.73, RMSE = 4.27°C)$	Sun et al., 2011

4. Results

4.1 Sediment analysis

4.1.1 Age-depth model

The Clam age-depth model (Fig. 2B) is based on ten calibrated ^{14}C dates (Table 1). Two ^{14}C dates (A2 86-87 at depth 195 cm and A6 91-92 at depth 597) were excluded from the age-depth model. The age-depth model constructed with the R 'Bacon' program (Blaauw and Christen, 2011; not shown) has rejected the two dates and the same information was used with the 'Clam' program. The VC2016 record extends from 9700 a cal BP to 800 a cal BP. The age-depth model has an error of ~50–260 years between 15-550 cm and ~210–470 years for the base of the core (550-600 cm) (Fig. 2B and Supplementary Table S5). The age–depth curve shows a sedimentation rate (16.7 cm.100 yr^{-1}) that decreases at 7560 a cal BP (3.3 cm.100 yr^{-1}) except between 5100 and 4950 a cal BP (43.5 cm.100 yr^{-1}). From the base of the core to 43 cm depth, an average temporal resolution of 77 years was achieved for pollen records and 202 years for brGDGTs.

4.1.2 Lithology changes

The core lithology is divided into 3 units (Fig. 2B). Unit 1 (600-558 cm) is characterized by a light gray clay and sand sediment. Unit 2 (558-170 cm) is composed of a gray clay sediment. Unit 3 (170-15 cm) is divided into 4 subzones. Unit 3a (170-144 cm) is composed of a brown peat silt sediment. Unit 3b (144-125 cm) is characterized by alternating yellow and dark peat silt sediments. Unit 3c (125-113 cm) is marked by a gray clay sediment. Unit 3d (113-15 cm) is composed of a peat silt sediment with brown, dark and orange colors. The clay sediments are interpreted as open underwater environments while the peat sediments indicate the accumulation of plant remains growing in place in restricted underwater or near-surface environments.

4.1.3 Geochemical composition

A principal component analysis (PCA) was conducted on XRF elements (Fig. 2B) and the sample map was colored according to the lithology units. The first two dimensions (PCA 1_{XRF} and PCA

2_{XRF}) explain 80% of the variability (64% and 16% respectively). Two major geochemical end-members are identified: the first one represents terrigenous inputs (K, Al, Mg, Si, Ti, Fe) and are positively correlated with PCA 1_{XRF}. Terrigenous elements are associated with clay sediments (Units 1 and 2) deposited in open underwater environments, and are opposed to organic sediments (Unit 3) mainly composed of peat sediments formed in restricted underwater or near-surface environments.

The second end-member represents carbonate components (Ca), sulfur (S) and phosphorus (P) and are positively correlated with PCA 2_{XRF}. Calcium is abundant at the base of the core (Unit 1) and in the first organic levels (Units 3a, 3b, 3c). Sulfur and phosphorus are only abundant in the first organic levels (Units 3a, 3b, 3c). The upper part of the core (Unit 3d) is distinguished by a biogenic silica production, visible in the ratio Si/Ti (Brown et al., 2007).

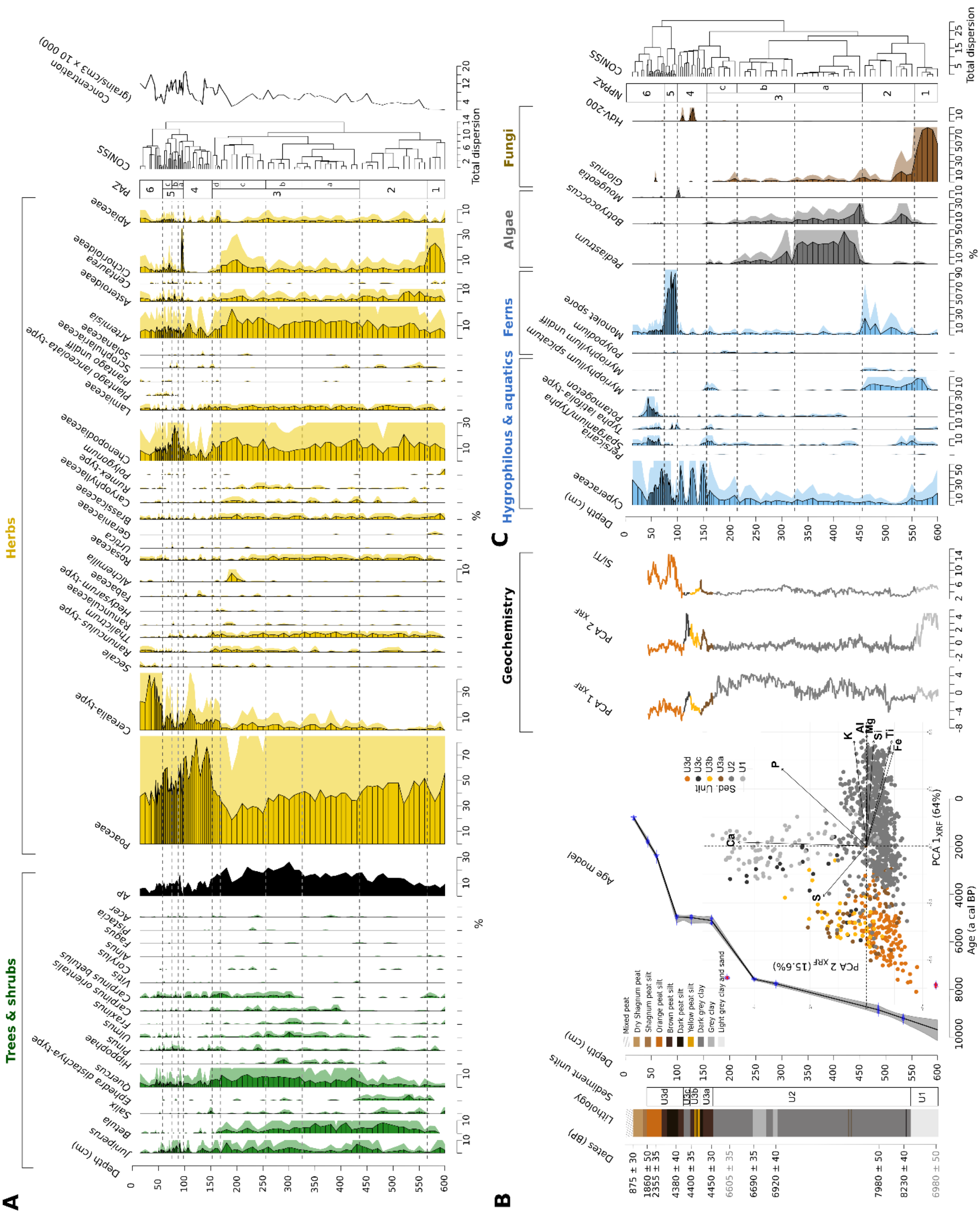

Figure 2. Pollen and sedimentology of Vanevan peat against core depth. A) Selected terrestrial pollen taxa. Tree, shrub, and herb pollen taxa are expressed in percentages of total terrestrial pollen. AP: Arboreal Pollen. PAZ: Pollen Assemblage Zones. B) Sediment lithology, age-depth model and geochemical data. The age–depth model is based on calibrated radiocarbon ages (with 2 σ errors) (AMS, see Table 1). Principal component analysis (PCA) was done on XRF data according to the lithological units. The first two dimensions (PCA 1_{XRF} and PCA 2_{XRF}) of PCA are arranged by depth. C) Selected hygrophilous and aquatic pollen taxa and NPPs. Hygrophilous and aquatic pollen taxa are expressed in percentages of total pollen. Fern spores, algae and fungi are expressed in percentages of total terrestrial pollen and NPPs. NPPAZ: Non-Pollen Palynomorph Assemblage Zones.

4.2 Pollen analysis and pollen-based climate reconstruction

4.2.1 Surface samples, vegetation, and climate

The modern pollen assemblages (Fig. 3) are dominated by herbaceous pollen taxa, including Poaceae, Chenopodiaceae and *Artemisia*. By comparing the pollen data with the vegetation, it appears that Poaceae is well associated with the local vegetation, while Chenopodiaceae, *Artemisia*, Asteroideae and Cichorioideae are over-represented. Arboreal taxa such as *Hippophae* is well associated with the local vegetation while *Quercus* and *Pinus* are over-represented.

The altitudinal vegetation gradient is well recorded in the modern pollen rain. The lower and middle elevations (800-1900 m) are dominated by pollen of Chenopodiaceae (33%), Poaceae (19%), *Artemisia* (16%), and indicate a semi-desert or steppe vegetation. A few pollen grains of *Pistacia* and *Salix* are also recorded. These levels are distinguished by high percentages of Chenopodiaceae and *Artemisia* and by low percentages of arboreal pollen taxa (7%). The upper elevations (1900-2300 m) record high percentages of Poaceae (30%), characteristic of meadow steppes, except when trees or shrubs are present in the local (*Hippophae, Salix, Juniperus, Acer, Viburnum*) or extra-local vegetation (*Pinus*). *Pinus* was present in the extralocal vegetation of sites number 13 and 18. However, only site number 13 records *Pinus* pollen. *Quercus*, *Carpinus betulus* and *Fagus* are recorded with low percentages (<4%). *Artemisia* and Chenopodiaceae represent only 7% and 4%, respectively. The subalpine and alpine environments are dominated by Poaceae pollen (38%) and few arboreal pollen taxa, such as *Quercus* (7%), *Betula* (6%), *Ulmus* (3%), are recorded. At these elevations, *Artemisia* and Chenopodiaceae represent 7% each.

Although the modern sites are distant from agricultural areas, pollen of *Cerealia*-type are recorded, reaching up to 11%. Pollen indicator of pastoralism activities, such as *Plantago lanceolata*-type or *Rumex*-type, represent less than 1% on average and a maximum of 6%. Otherwise, the pollen rain shows correspondence to climatic gradients (Fig. 3). The highest percentages of Chenopodiaceae and *Artemisia* pollen correspond to high temperature (>5°C) and low precipitation (MAP<500 mm). The limit between cool and warm steppe biomes correspond to a change in Chenopodiaceae percentages and in MAP. In contrast, percentages of Poaceae pollen increase when MAAT decreases.

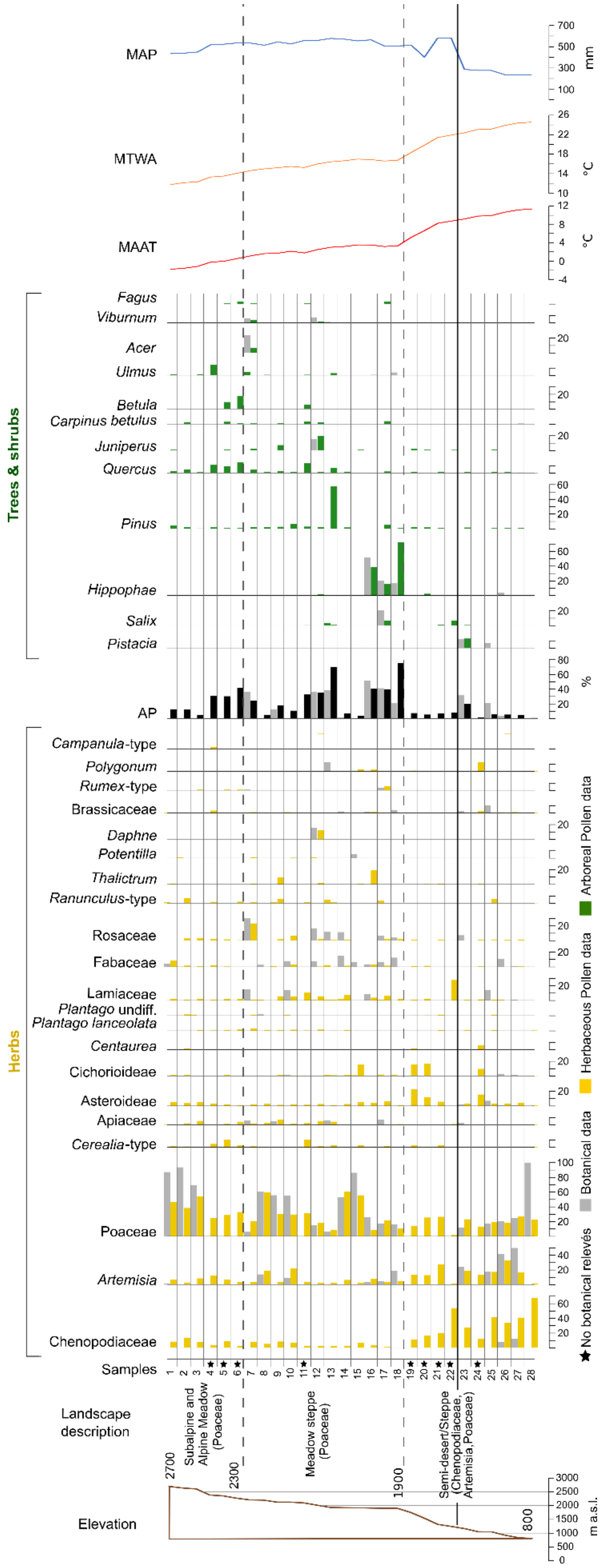

Figure 3. Selected modern pollen assemblages, botanical relevés and climate values along an altitudinal transect in Armenia. MAAT=mean annual air temperature, MTWA= mean temperature of the warmest month, MAP= mean annual precipitation.

4.2.2 Pollen sequence: terrestrial, hygrophilous vegetation, and Non-Pollen Palynomorphs

A total of 76 terrestrial pollen taxa were identified in the Vanevan core VC2016. Herbaceous pollen taxa dominate the pollen assemblages along the sequence ranging from 73 to 99%. The pollen diagram is divided into 6 pollen assemblage zones (PAZ) according to the CONISS method (Grimm, 1987) and visual differences for subzones transitions (PAZ 3a/3b) (Fig. 2A, Table 3). The diagram of NPPs and hygrophilous vegetation is divided into 6 Non-Pollen Palynomorph assemblage zones (NPPAZ) according to the CONISS method (Grimm, 1987) (Fig. 2C, Table 3). The limits of NPPAZ generally follow changes in lithology.

Table 3. Inventory of pollen assemblage zones (PAZ), depth, estimated ages, total of arboreal pollen (AP_t), common and rare pollen types (CPT, RPT) for arboreal and herbaceous taxa, Non-Pollen Palynomorph assemblage zones (NPPAZ) and main hygrophilous pollen taxa and Non-Pollen Palynomorphs (NPPs). Common pollen types (CPT) include pollen taxa with percentages > 5% and rare pollen taxa (RPT) percentages < 5%

PAZ	Depth (cm) *Age (a cal BP)*	Total of Arboreal Pollen %	Arboreal and herbaceous pollen Common pollen types (CPT) Rare pollen types (RPT)	NPPAZ	Hygrophilous pollen NPPs
6	58-15 *2350-790*	AP_t 7	CPT: Poaceae, *Cerealia*-type, Chenopodiaceae, *Artemisia* RPT: Cichorioideae, Asteroideae, Apiaceae Rosaceae, *Ranunculus*-type, *Quercus, Carpinus betulus, Juniperus*	**6**	Cyperaceae, *Potamogeton, Sparganium/Typha,* Cyperaceae
5c	76-58 *3500-2350*		CPT: Poaceae, Chenopodiaceae, *Cerealia*-type, *Artemisia* RPT: Cichorioideae, Asteroideae, Apiaceae; *Quercus, Juniperus, Carpinus betulus, Pinus*		
5b	88-76 *4300-3500*		CPT: Poaceae, Chenopodiaceae, *Artemisia, Cerealia*-type RPT: Asteroideae, Cichorioideae, Apiaceae, *Juniperus, Quercus, Pinus, Carpinus betulus*		
5a	98-88 *4950-4300*		CPT: Poaceae, Cichorioideae, Chenopodiaceae, *Artemisia* RPT: *Cerealia*-type, Asteroideae, Lamiaceae, *Thalicthrum; Quercus, Juniperus, Pinus, Carpinus betulus*		
5	98-58 *4950-2350*	AP_t 9		**5**	Monolete spores, *Typha latifolia*-type, Cyperaceae
4	153-98 *5100-4950*	AP_t 8	CPT: Poaceae, *Cerealia*-type, Chenopodiaceae, *Artemisia* RPT: Lamiaceae; *Quercus, Juniperus, Carpinus betulus*	**4**	Alternating episodes with or without Cyperaceae accompanied by *Sparganium/Typha, Myriophyllum spicatum,* fungi HdV-200, *Mougeotia*
3d	256-153 *5200-5100*		CPT: Poaceae, Chenopodiaceae, *Cerealia*-type, *Artemisia* RPT: Cichorioideae, Asteroideae, *Quercus, Carpinus betulus, Juniperus, Carpinus orientalis*		
3c	256-169 *7600-5200*		CPT: Poaceae Chenopodiaceae, *Artemisia, Cichorioideae, Quercus, Alchemilla* RPT: *Cerealia*-type, Asteroideae, *Thalictrum,* Brassicaceae, Lamiaceae, Rosaceae, *Ranunculus*-type, *Caryophyllaceae, Rumex*-type; *Betula, Juniperus, Carpinus betulus*		
3b	326-256 *8000-7600*		CPT: Poaceae, *Artemisia,* Chenopodiaceae, *Quercus* RPT: *Cerealia*-type, *Thalictrum,* Cichorioideae, Brassicaceae, Apiaceae, Lamiaceae, Rosaceae, Asteroideae, *Caryophyllaceae, Ranunculus*-type,		

			Rumex-type*; Betula, Juniperus,Ulmus, Fraxinus, Hippophae, Carpinus betulus, Carpinus orientalis*		
3a	436-326 *8600-8000*		CPT: Poaceae, *Artemisia*, Chenopodiaceae RPT: *Cerealia*-type, *Thalictrum*, Cichorioideae, Brassicaceae, Apiaceae, Lamiaceae, Rosaceae, Asteroideae, *Caryophyllaceae*; *Betula, Quercus, Ulmus, Fraxinus, Carpinus orientalis, Hippophae, Pinus*		
3	436-153 *8600-5100*	AP_t 17	Maximum of arboreal pollen percentages and diversity. Progressive decrease in Poaceae and trees until 5900 a cal BP.	**3**	Planktonic algae (*Pediastrum, Botryococcus*), Cyperaceae
2	566-436 *9400-8600*	AP_t 13	CPT: Poaceae Chenopodiaceae, *Artemisia* RPT: *Cichorioideae*, Asteroideae, *Thalictrum*, Brassicaceae, Apiaceae, Lamiaceae, Rosaceae; *Betula, Quercus, Juniperus, Ephedra distachya*-type, *Salix, Hippophae*	**2**	*Myriophyllum spicatum*, Monolete spores. At 9200 a cal BP, peak of Botryococcus *Glomus, Sparganium/Typha*
1	600-566 *9700-9400*	AP_t 8	CPT: Poaceae, Cichorioideae, Chenopodiaceae *Artemisia* RPT: Asteroideae, *Polygonum, Thalictrum*, Brassicaceae, Apiaceae; *Juniperus, Quercus, Betula, Carpinus betulus*	**1**	*Glomus*, Cyperaceae, *Myriophyllum spicatum*

4.2.3 Comparison between surface and core samples

A classification by hierarchical cluster analysis was conducted on Armenian surface samples and core VD2016 samples (Fig. 4). The surface samples are well distributed within the core samples: the surface samples dominated by Poaceae (n. 1-3, 8, 14, 15), are close to core samples which record a large percentage of Poaceae (PAZ 1, 2, 4, 5) whereas those recording regional arboreal taxa (n. 4-7, 9-12, 17) approach the core samples of PAZ 3 representing the most forested phase. At lower and middle elevations, the surface samples with a large percentage of Cichorioideae (19, 20, 24) are close to the PAZ 1 core samples recording a large proportion of this taxon whereas those dominated by Chenopodiaceae, Artemisia and Poaceae (n. 13, 16, 18, 21-23, 25-28; i.e. mainly lowland samples) seem more different of the core samples.

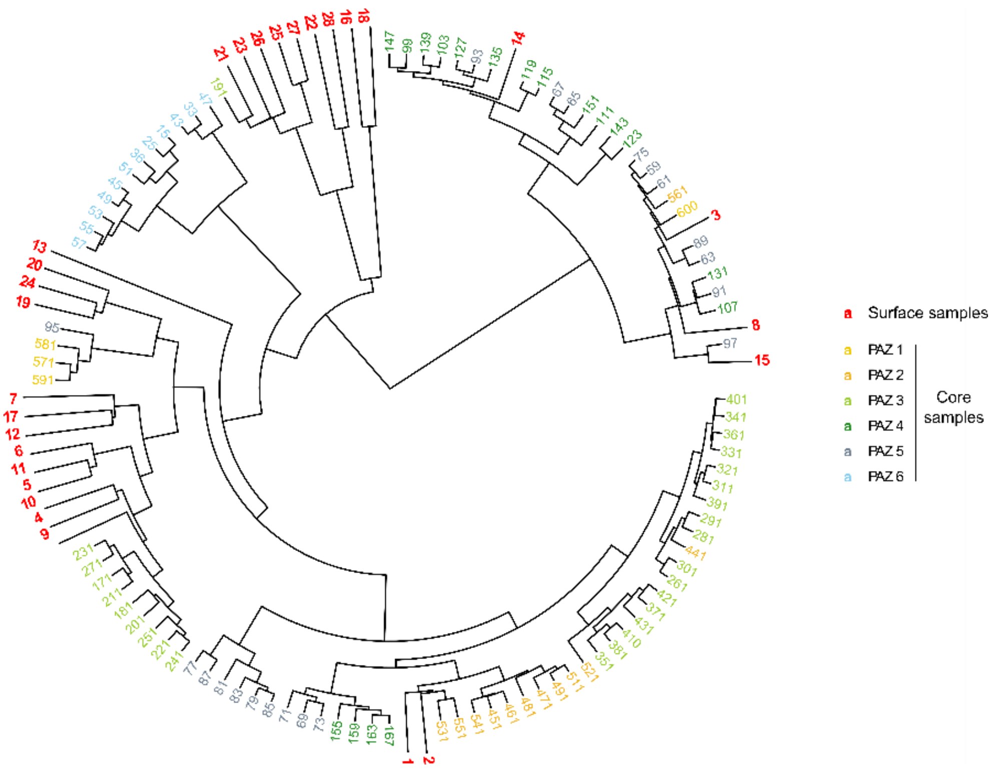

Figure 4. Classification by hierarchical cluster analysis on surface samples of Armenia (presented in Fig. 3) and core samples of VD2016 expressed in depth (presented in Fig. 2). The color of core samples corresponds to the six pollen assemblage zones (PAZ) defined with the CONISS method. The distance matrix was calculated using Euclidean distance and Ward's algorithm was applied for clustering.

4.2.4 Pollen-inferred climate reconstruction

Climate changes at Vanevan are estimated using four methods: MAT, WAPLS, RF, and BRT (Fig. 5). The climate patterns reconstructed are consistent and do not seem method-dependent. The MAT and the BRT appear as the most sensitive methods and the results show important sample-to-sample variability; the WAPLS method shows large variations along the Holocene and the inferred values are significantly higher than the modern values; the RF is the less sensitive method (Fig. 5). Correlations between current and estimated climate parameters show the maximum R^2 for the RF and BRT methods (Supplementary Fig. S3). However, the RF method does not reconstruct correctly the high or the low current climate values. Statistical results of the model performances are presented in Supplementary Table S4; the BRT method presents the maximum R^2 and the minimum RMSE for all climatic parameters.

Based on the multi-method approach, the Vanevan climate reconstruction (Fig. 5) shows remarkably consistent trends during the Holocene, except for the most recent periods. Five climatic phases have been defined and are described below.

Phase 1 (9700 – 8200 a cal BP) is first characterized by warm and wet conditions. For temperature and annual precipitation, all methods show the same trend although the reconstructed values can be different. Then, the reconstructions show a drop in temperature and precipitation with a minimum between 8600 and 8200 a cal BP.

Phase 2 (8200 – 5500 a cal BP) is marked by warmer conditions than previously. Temperatures increase and reach an optimum around 6000 a cal BP (2.5-6°C for MAAT and 17-19°C for MTWA). Considering precipitation, it first increases and then declines around 6000 a cal BP (350-530 mm/year for MAP and 130-150 mm/year for Psummer).

Phase 3 (5500 – 4300 a cal BP) shows cooler and wetter conditions than previously. Precipitation increases for all methods reaching 460-550 mm/year for MAP and 130-170 mm/year for Psummer.

Phase 4 (4300 - 3500 a cal BP) is mainly characterized by a drop in annual precipitation and particularly in Psummer with a minimum at 4100 a cal BP (90-150 mm/year).

Phase 5 (3500 - 800 a cal BP) is marked by divergent trends according to the methods. The MAT, RF, and BRT methods record a decrease of temperature and precipitation. In contrast, the WAPLS method shows the warmest and the wettest conditions of the Holocene. At 2800 a cal BP, a decrease in temperature and precipitation are recorded by WAPLS and RF methods.

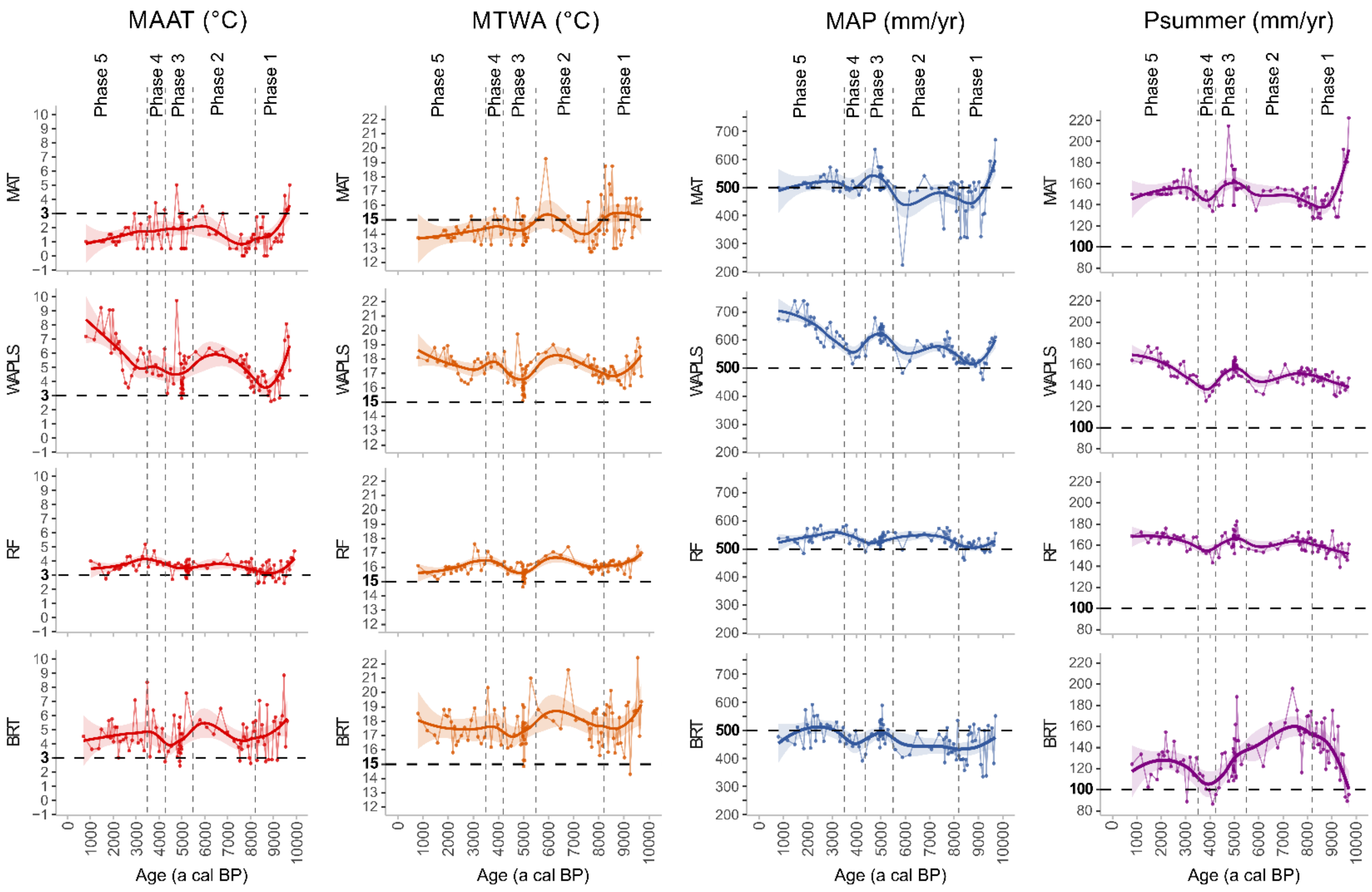

Figure 5. Pollen-inferred climate changes estimated using four methods: MAT (Modern Analogue Technique), WAPLS (Weighted Averaging Partial Least Squares regression), RF (Random Forest) and BRT (Boosted Regression Trees). Dotted lines correspond to modern values (Sevan city meteorological station). MAAT: mean annual air temperature. MTWA: mean temperature of the warmest month. MAP: mean annual precipitation. Psummer: summer precipitation.

4.3 GDGT analysis

4.3.1 Distribution of brGDGTs

The concentration of brGDGTs (Fig. 6D) ranges from 0.04 to 11.6 µg/g dry sediment. The fractional abundances of brGDGTs (Fig. 6A) show a dominance of pentamethylated brGDGTs (II, 49%) in particular brGDGT IIa (20%), brGDGT IIa' (11%), and brGDGT IIb (9%). The relative abundance of tetramethylated brGDGTs (III, 26%) is explained by the abundance of brGDGT Ia (14%) and brGDGT Ib (10%). Finally, the relative abundance of hexamethylated brGDGTs (III, 25%) can be explained by the presence of brGDGT IIIa (11%) and brGDGT IIIa' (9%). The relative abundances of tetra, penta- and hexamethylated brGDGTs (Fig. 6B) differ according to the type of sediment in the core. The peat sediment samples are close to global soils and peats, whereas the clay sediment samples are closer to global lakes.

A principal component analysis (PCA) and a hierarchical clustering on principal components (HCPC) were conducted on the fractional abundances of brGDGTs with *FactoMineR 2.4* package (Lê et al., 2008) (Fig. 6C). The first two dimensions (PCA 1 and PCA 2) explain 86% of the variability (54% and 32% respectively). Three groups are identified by HCPC: the first one is associated with tetramethylated brGDGTs and the samples are negatively correlated with PCA 1. This group is composed of peat sediment samples. The second one is associated with brGDGTs ΣIIa and the samples are negatively correlated with PCA 1 and PCA 2. The group is composed of samples mainly located in the lithological transition zone of the core between peat and clay sediments. The third one is associated with hexamethylated brGDGTs, brGDGTs ΣIIb and brGDGTs ΣIIc and the samples are positively correlated with PCA 1. The group is mainly composed of lake-type sediment samples.

4.3.2 Ratio and indices

The ΣIIIa/ΣIIa ratio shows a general decreasing trend from the beginning to the end of the core (Fig. 6D). From 9700 to 5100 a cal BP (lake sediment), the average ΣIIIa/ΣIIa ratio is equal to 0.83 and then from 5100 a cal BP to today (peat sediment), the average ratio is equal to 0.52. The MBT and the MBT'5Me show similar variations but different absolute values (Fig. 6D). The MBT varies between 0.15 and 0.40 and the MBT'5Me between 0.30 and 0.51. From 9700 to 7300 a cal BP, the index values increase and then remain relatively stable. From 7300 a cal BP, they decline and from 5000 a cal BP they largely increase. From 4200 to 3000 a cal BP, the index values progressively decrease and then remain stable except at 1800 a cal BP. The CBT index shows variation between 0.17 and 0.42 except at 9200, 8900 and 5000 a cal BP where the values vary from 0.5 to 0.71 (Fig. 6D).

4.3.3 Temperature reconstructions

The reconstructed mean annual air temperature (MAAT) using soil (Naafs et al., 2017a) and lake calibrations (Sun et al., 2011) show similar trends but different absolute values (Fig. 6D). For soil, the average MAAT is equal to 0.66 °C during the Holocene and for lake the average MAAT is equal to 11.9 °C. Between 9700 to 7300 a cal BP, MAAT reconstructed values increase and then remain relatively stable. For this period, the average MAAT is equal to 10.4 °C for lake calibration. From 7300 a cal BP, the MAAT reconstructed values decline, reaching 9.6°C for lake calibration at 6200 a cal BP. Then shifting to soil calibration, a large increase is recorded from 5000 a cal BP and the MAAT reaches 5.7°C. From 4200 to 3000 a cal BP, the MAAT progressively decrease and then remains stable until the present at around 0.86°C for soil calibration except at 1800 a cal BP when a peak is recorded. The ΔMAAT records low temperatures between 9700 and 8700 a cal BP and a plateau until 7400 a cal BP followed by a continuous decrease onward. Inner variability in this last trend occurs at 4900-3600 a cal BP and a single peak at 1800 a cal BP.

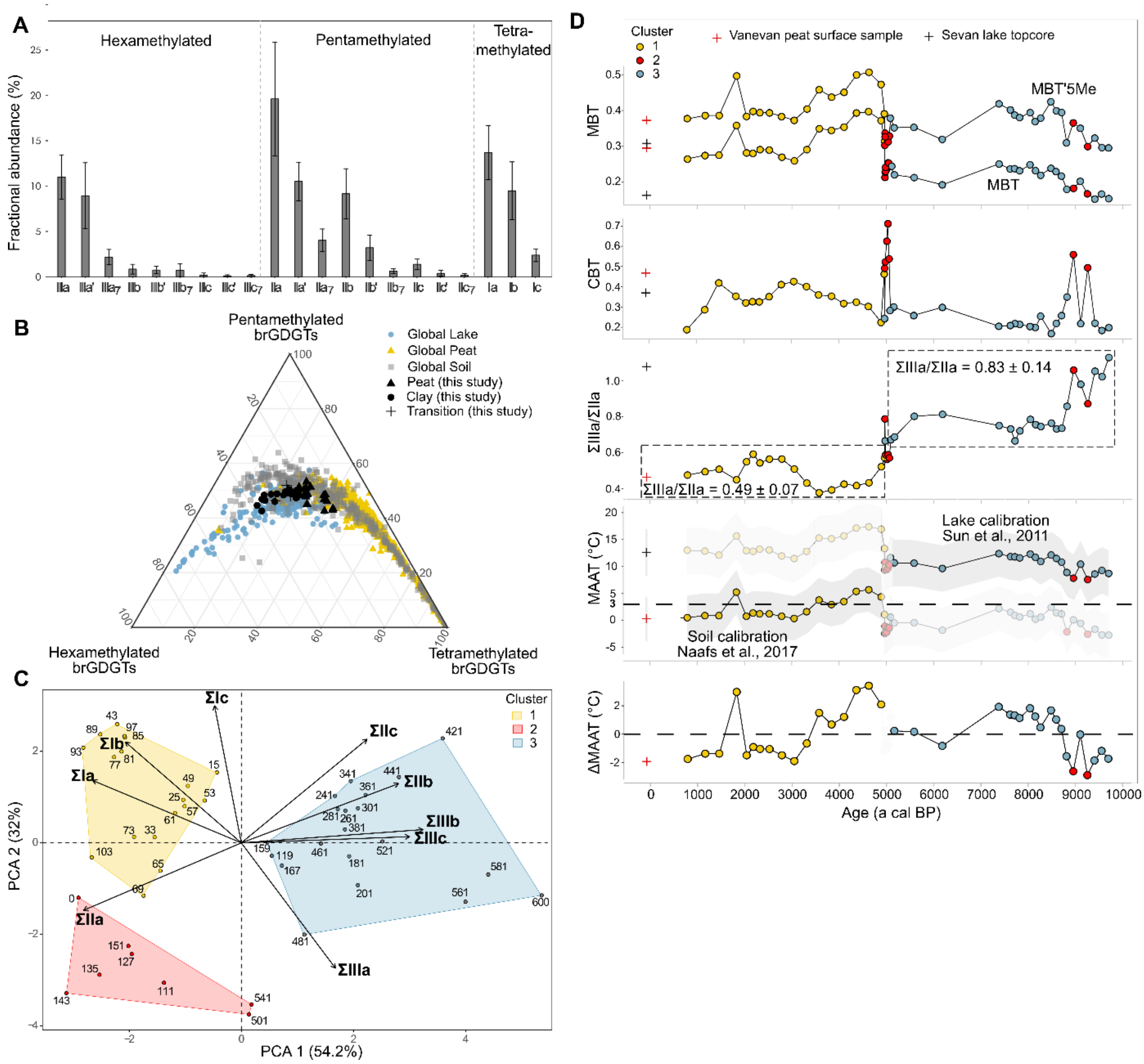

Figure 6. A) Average fractional abundance of individual brGDGT, B) Ternary diagram showing the fractional abundances of tetra-, penta-, and hexamethylated brGDGTs. The dataset of Vanevan core are plotted against that of lakes (Wang et al., 2012; Günther at al., 2014; Li et al., 2016; Zink et al., 2016; Dang et al., 2018; Weber et al., 2018; Martin et al., 2019; Ning et al., 2019), of global peat (Naafs et al., 2017b), and of soils (Yang et al., 2014;

Naafs et al., 2017a). C) Principal component analysis (PCA) and hierarchical clustering on principal components (HCPC) with fractional abundances of brGDGTs. Labels correspond to sample depth. D) Degree of methylation (MBT, MBT'5Me), Cyclisation ratio (CBT), ΣIIIa/ΣIIa ratio, Mean annual air temperature values (MAAT) based on Naafs et al., 2017a and Sun et al., 2011, Difference of temperature (ΔMAAT) against age. ΔMAAT corresponds to the centered values based on the mean value of the two sediment types (peat and lake).

5. Discussion

5.1 Pollen representation in modern vegetation and relationship with climate variables

The relationship between pollen assemblages and modern vegetation depends on various factors, including pollen production, type of pollination, dispersion mechanisms, surrounding vegetation, topography and microclimatic parameters (Jacobson and Bradshaw, 1981). Pollen rain integrates local to regional vegetation (Jacobson and Bradshaw, 1981; Prentice, 1985). In Armenia, the vegetation is largely open which contributes to a greater pollen dispersion, but topography and microclimatic parameters may also play significant roles. Understanding the representation of pollen and their origins are important for the reliability of the fossil record in vegetation and climate reconstructions.

In our study (Fig. 3), the modern vegetation shows the dominance of herbaceous taxa whose pollen representation largely depends on the type of pollination. The insect-pollinated nature of Fabaceae and Rosaceae explain their under-representation whereas the wind-pollinated nature of Asteraceae (*Artemisia*, Asteroideae and Cichorioideae) and Chenopodiaceae explain their over-representation (Fig. 3). These results are consistent with previous studies in semi-arid regions of the Caucasus where Chenopodiaceae represent 30% to 80 % of the pollen signal (Connor et al., 2004). In the desert regions of East Asia, Chenopodiaceae is the most abundant taxa and represents more than 60% of the pollen signal in China (e.g. Zhao and Herzschuh, 2009; Wei and Zhao, 2015; Zhang et al., 2018) and Mongolia (Ma et al., 2008). *Artemisia*, another taxa characterizing the semi desert-steppe environments of Armenia, is associated with the local vegetation along our sample gradient but is also present without local presence (Fig. 3), indicating over-representation. This is consistent with observations from the arid and semi-arid areas of Iran (up to 80% of the pollen signal in Djamali et al., 2009), China (e.g. Li et al., 2005; Xu et al., 2007, 2009; Zhang et al., 2018), and Mongolia (Ma et al., 2008) where *Artemisia* is the dominant taxa in steppe regions. In contrast, in Georgia (Connor et al., 2004) and Armenia, *Artemisia* is never the dominant taxa in modern pollen assemblages, although it is well recorded in semi desert-steppe environments of Armenia. According to previous studies in East Asia (e.g. Li et al., 2008; Zheng et al., 2008), the over-representation of Chenopodiaceae and *Artemisia* could be explained by wind transport dispersal, their long-distance transport capacity and a high pollen production. In our study, Chenopodiaceae and *Artemisia* are registered in all modern samples although they are not necessarily present in the local vegetation. Chenopodiaceae is even well registered in subalpine and alpine meadows whereas they do not appear in the vegetation, confirming the previous assumptions.

In steppes, subalpine and alpine meadows of Armenia, Poaceae is the dominant taxa and it is reliably associated with the local vegetation (Fig. 3). In East Asia, Poaceae is very common in the semi-desert and steppe vegetation, even though it is generally not the dominant taxa in pollen assemblages due to under-representation (e.g. Ma et al., 2008; Xu et al., 2014). However, in protected areas of Mongolia, Poaceae is better recorded in pollen assemblages (Ma et al., 2008). Anthropogenic activities, such as overcultivation and overgrazing, may prevent the flowering of Poaceae plants (Ma et al., 2008; Wei and Zhao, 2015). The rapid deterioration of Poaceae pollen after their deposition may also contribute to the low representation of Poaceae in pollen assemblages of soils and mosses (Cao et al., 2007). In general, Poaceae is under-represented in pollen assemblages and often represents a quarter of vegetation (Ge et al., 2017). However, our study and Connor et al. (2004) show that in Georgia and Armenia, Poaceae is well associated with the vegetation. In our case, the p/v ratio (average pollen percentages/average vegetation cover percentages) is equal to 0.99, indicating a good correspondence between pollen and local vegetation. The reliable representation of Poaceae could be explained by the abundance of Poaceae in Armenia and a limited anthropogenic pressure with extensive pastoralism.

Anthropogenic indicators, such as *Plantago lanceolata* and *Rumex*-type are present in very low proportion even with extensive pastoralism which is not easily detectable in the modern pollen assemblages. Considering *Cerealia*-type, the pollen percentages are low and no relationship was found between pollen and vegetation. These results are consistent since the selection of modern sites was done in areas remote from agricultural zones.

Arboreal pollen taxa are registered in all modern samples, but they are mainly present at mid- and high elevations (Fig. 3). In meadow steppes, trees and shrubs come primarily from local or extra-local vegetation whereas in subalpine and alpine meadows, trees come from regional vegetation. The long-distance component varies depending on the location and the elevation of modern sites and it also favored by the vegetation openness in Armenia. Arboreal pollen taxa representative of the local vegetation are *Hippophae*, *Pistacia*, *Salix*, *Juniperus*, *Acer* and *Viburnum*. In semi desert-steppe environments, *Pistacia* can be present in areas close to sparse arid woodlands. In meadow steppes, *Hippophae* is present in areas close to humid zones (Lake Sevan, rivers), *Salix* in riparian areas and *Juniperus* on south-facing slopes. In the sample from the Lake Sevan surrounding, *Hippophae* is well associated with the local vegetation even if it is a wind-pollinated tree (Li et al., 2005).

Other trees (*Pinus*, *Quercus*, *Carpinus betulus*, *Betula*, *Ulmus* and *Fagus)* recorded in our samples come from regional vegetation. Their over-representation may be partly explained by a wind pollination. *Pinus* pollen is registered at all elevations even if it is not present in the vegetation, except around Lake Sevan. There, *Pinus* was planted during afforestation program of USSR in the eighties. However, these pine plantations do not seem to produce pollen, as indicated by the low percentages of *Pinus* for the sample 18. A similar result occurs around the Mount Aragats in Armenia where *Pinus* is poorly registered despite the presence of planted pine trees for approximately 40 years (Cromartie et al., 2020). *Pinus* is considered as a high pollen producer and it has a good pollen dispersion by wind (Connor et al., 2004). In subalpine and alpine meadows, *Quercus* pollen averages 7% when oak forests are not present. Interestingly, oak pollen is recorded at the same elevations inhabited by oaks on the reverse slopes of the northeast mountains of Armenia and Azerbaijan. The over-representation of *Quercus* is also reported from Georgia (Connor et al., 2004) and Iran (Ramezani et al., 2013) although *Quercus* has a good pollen representation in the eastern part of Iran (Djamali et al., 2009). *Quercus* is a high pollen producer and it is often well represented in the modern pollen assemblages of the Near East (Connor et al., 2004). Our study confirms that *Quercus* pollen can be transported over long distance, even where topographic barriers are high.

The relationship between modern pollen assemblages and climate variables is marked across the altitudinal transect. Chenopodiaceae and *Artemisia* pollen dominate in semi desert-steppe vegetation of Armenia when MAAT is high and MAP is low whereas Poaceae are dominant in meadow steppes, subalpine and alpine meadows when MAAT decreases. Chenopodiaceae and *Artemisia* are indicators of continental climate characterized by cold winters and dry summers (El-Moslimany, 1990). In the Near East and Asia, the *Artemisia*/Chenopodiaceae (A/C) ratio is used as an aridity index for desert and steppe environments (e.g. Herzschuh, 2007; Zhao and Herzschuh, 2009). However, in Georgia a low relationship between A/C ratio and precipitation is observed compared to Chenopodiaceae percentages alone (Connor et al., 2004). In our study, Chenopodiaceae dominance also has higher relationship to MAP (R^2=0.40) and MAAT (R^2=0.58) than A/C ratio to MAP (R^2=0.02) and MAAT (R^2=0.16). In the South Caucasus, Chenopodiaceae changes seem to be a better aridity index than the A/C ratio.

5.2 Holocene reconstruction at a local scale: wetland dynamics and human activities at Vanevan

5.2.1 Validation of age-depth model

The comparison of the vegetation dynamics with that of the closest site (Shenkani, Cromartie et al., 2020) validates the age model. Similar trends are observed in both sites: occurrence of *Carpinus betulus* from 9700 to 9300 a cal BP, *Betula* beginning at 9600 a cal BP (Fig. 7), an arboreal taxa maximum at 7800 a cal BP, and a drop of *Betula* at 5000-4700 a cal BP.

At Vanevan, however, the trends evidenced in cores VD2016 (this study) and VD2011 (Leroyer et al., 2016) are closely related but changes are not simultaneously (Supplementary Fig. S6). For example, the maximum of arboreal pollen dates to 7800 and 6800 a cal BP for VD2016 and VD2011, respectively. Similarly, both sequences end with a peak of arboreal pollen at 5900 and 5600 a cal BP for VD2011 and VD2016 followed by an increase of Poaceae, Cyperaceae, and then ferns at 5100 and 4900 a cal BP for VD2011 and VD2016. This comparison therefore reveals a temporal gap between the two cores ranging from 2200 years at the base to 300 years at the top of the VD2011 sequence. Underestimation of the ages in the VD2011 sequence could be explained by an age model based on plant macrofossils imbedded in clay sediments. It should, moreover, be noted that the most basal date of VD2011 core, rejected by the authors, is consistent with the older ages of the VD2016 core.

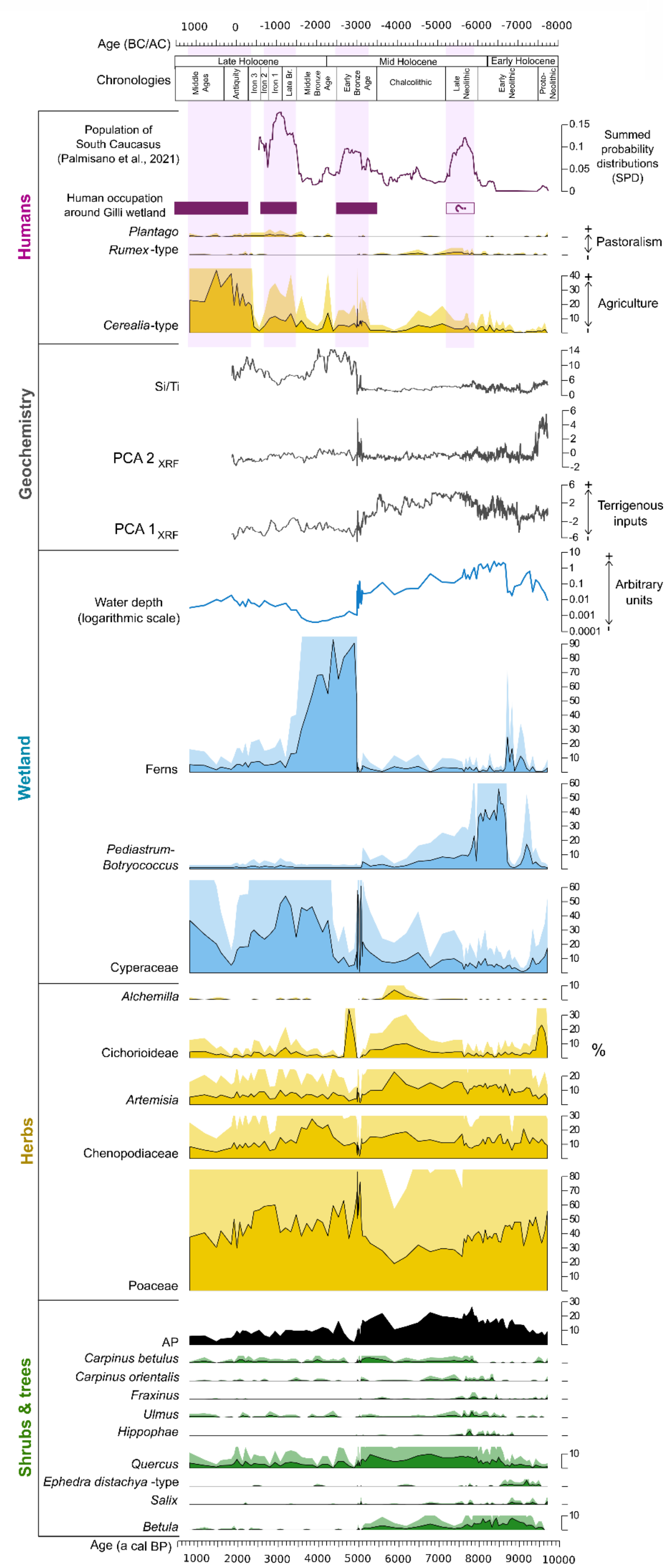

Age (BC/AC)
1000
0
-1000
-2000
-3000
-4000
-5000
-6000
-7000
-8000
Chronologies
Late Holocene
Mid Holocene
Early Holocene
Middle Ages
Antiquity
Iron 3
Iron 2
Iron 1
Late Br.
Middle Bronze Age
Early Bronze Age
Chalcolithic
Late Neolithic
Early Neolithic
Proto-Neolithic
Humans
Population of South Caucasus (Palmisano et al., 2021)
Summed probability distributions (SPD)
Human occupation around Gilli wetland
Plantago
Rumex -type
Pastoralism
Cerealia-type
Agriculture
Geochemistry
Si/Ti
PCA 2 XRF
PCA 1 XRF
Terrigenous inputs
Wetland
Water depth (logarithmic scale)
Arbitrary units
Ferns
Pediastrum-Botryococcus
Cyperaceae
Herbs
Alchemilla
Cichorioideae
%
Artemisia
Chenopodiaceae
Poaceae
Shrubs & trees
AP
Carpinus betulus
Carpinus orientalis
Fraxinus
Ulmus
Hippophae
Quercus
Ephedra distachya -type
Salix
Betula
Age (a cal BP)
1000
2000
3000
4000
5000
6000
7000
8000
9000
10000

734

Figure 7. Selected Pollen taxa, NPPs, XRF, and archeological data of Vanevan peat against age. Water depth = (Algae+1)/(semi-aquatic plants+1))/(ferns +1) plotted on a logarithmic scale. Algae: *Pediastrum*, *Botryococcus*. Semi-aquatic plants: Cyperaceae, *Sparganium*, *Typha*. Ferns: Monolote spore, *Botrychium*, *Polypodium*, *Selaginella*, *Asplenium*.

5.2.2 Wetland dynamics and water-level changes

Aquatic taxa, fern spores, and NPP variations are environmental indicators of the type of wetland, the openness of the waterbody, and its water depth. Following Joannin et al. (2012), a ratio between such environmental indicators is used to estimate changes in water-level (Fig. 7), and for comparison with the conditions indicated by the lithology and XRF data. The ratio increases from 9700 to 8600 a cal BP, progressively decreases until 5100 a cal BP and remains low afterwards.

From 9700 to 5100 a cal BP, the Vanevan sequence is characterized by clay sediments formed by inputs of detrital elements (PCA 1_{XRF}, Fig. 7). The poorly developed semi-aquatic vegetation and the presence of freshwater algae suggest a lake system seen in the water-depth reconstruction. This is consistent with a transgression of Lake Sevan reported in Sayadyan's works (1977-1983). Within this period, however, we can distinguish a low water-level phase from 9700 to 9400 a cal BP consistent with the regressive phase reported by Sayadyan (1977-1983) at the same period. Such conditions would create an erosional context and may explain both the dominance of the mycorrhizal root-fungi *Glomus* (Fig. 2C) and high calcium concentrations (PCA 2_{XRF}, Fig. 7). *Glomus* is often interpreted as an indicator of close distance soil-related input (Wünnemann et al., 2010; Mudie et al., 2011) and the proportion of calcium may be derived from evaporative concentration, biogenic production (Cohen, 2003) or dissolution of the basaltic outcrops around or in the lake (detrital or in situ; Gudbrandsson et al., 2011). This raises the question of whether the calcium recorded in Vanevan was produced during the regression phase or produced before and washed down during this phase. According to Sayadyan (2009), Lake Sevan was high at the onset of the Holocene and it could have been connected with the Gilli wetland. As calcium concentrations were high in Lake Sevan before the Soviet lowering (Alekin and Ulyanova, 1986), it could be due to the remobilization of previous carbonates formed during a high stand of the paleoSevan. The high percentages of Cichorioideae also fit in a regression scenario as it is not connected to known regional vegetation development and therefore suggest local development or taphonomic processes in erosive conditions leading to an over-representation of this resistant pollen taxa (Lebreton et al., 2010).

A transitional phase is recorded between 5100 and 4950 a cal BP and shows large variations in Cyperaceae percentages. Succesive peaks of the saprophyte fungi HdV-200 may indicate alternating drying conditions followed by aquatic phases (Kuhry, 1985; van Geel et al., 1989). A peak of the green algae *Mougeotia* (Zygnemataceae) is recorded and may indicate changes in the trophic conditions and could play a role in the water-plant succession (Van Geel and van der Hammen, 1978; Van Geel and Grenfell, 1996). This phase is also characterized by high proportions of calcium, sulfur and phosphorus (PCA 2, Fig. 7) and corresponds to high fire activity (core VD2011, Leroyer et al., 2016; Supplementary

Fig. S6). The macrocharcoals reported in Leroyer et al. (2016) are assumed to reconstruct local scale fires and the chemistry of the fire byproducts is likely recorded through the XRF data (Smith, 1969). The fire activity seems to have burned Cyperaceae sedges or grassland and favored developments of ferns and Poaceae. The same vegetation dynamic after fire events are recorded at Shenkani (Cromartie et al., 2020). In the Vanevan wetland, the ecological perturbation of fire also results in a brief but massive peak of Cichorioideae recorded at 4800 a cal BP. Again, the presence of this taxa suggests a local development on perturbed soil or a drying phase leading to an over-representation of the resistant pollen taxa (Lebreton et al., 2010). The relative impact of human activities and climate changes on the rapid water-level fluctuations between 5100 and 4800 a cal BP remains to be determined because agricultural activities are present around Gilli wetland and climate changes are recorded at this period in the region.

After 4800 a cal BP, the Vanevan wetland then evolves towards a peatland characterized by peat deposits produced by a semi-aquatic vegetation, primarily Cyperaceae. The water level is low until 4500 a cal BP before the development of semi-aquatic vegetation. Abundant ferns are associated with the increase of the ratio Si/Ti. The biogenic silica production is likely due to phytoliths associated with the ferns (Brown et al., 2007). The water-level remains low and the wetland is dominated by Cyperaceae, except from 2300 to 1800 a cal BP when *Potamogeton*, *Sparganium* and *Typha* dominated the signal (Fig. 2C). This corroborates the Lake Sevan transgression (through underground influence) dating from 2350 to 1700 a cal BP (Sayadyan et al., 1977; Sayadyan, 1978, 1983). In Armenia, a water-level rise is also registered at Shenkani between 2200 and 1500 a cal BP (Cromartie et al., 2020).

5.2.3 Human impact

Agriculture

In our record, human activities are principally expressed through agricultural practices identified by *Cerealia*-type pollen. Although, *Cerealia*-type pollen may come from Poaceae species or wild cereals commonly present in the Near East (Van Zeist et al., 1975), our record matches the estimates of the population in the South Caucasus (Fig. 7) (Palmisano et al., 2021).

Low percentages of *Cerealia*-type pollen are recorded between 8300 and 6300 a cal BP (Late Neolithic-Chalcolithic). However, there is limited evidence of a Neolithic presence around Vanevan during this period evidenced only by an obsidian source, (Khorapor) located ~20 km away from the Vanevan peatland, which may have been used by Neolithic populations (Chataigner and Gratuze, 2014). Some evidence of Neolithic occupations is also recorded in the Kasakh valley, ~50 km from Lake Sevan (Colonge et al., 2013) and agriculture during this period is primarily recorded on the Ararat plain at an elevation of 850 m a.s.l. (Badalyan et al., 2004; Hovsepyan and Willcox, 2008; Badalyan and Harutyunyan, 2014). During the Early and Middle Chalcolithic, the archeological site of Getahovit-2 in north-eastern Armenia shows the presence of cereals. According to Chataignier et al., 2020, cereals were not locally cultivated (Chataignier et al., 2020), however, such a transport of cereals at this period is not evidenced around the Lake Sevan. The presence of *Cerealia*-type pollen in our record questions the conservation of archeological remains on the shores of Lake Sevan. The high degree of mobility of Neolithic population (Ricci et al., 2018) has certainly not helped to the conservation of archeological material.

Since 5200 a cal BP, archeological remains and *Cerealia*-type pollen occur simultaneously when the environmental conditions shift from a lake to a peatland due to an abrupt drop of water level.

Percentages of *Cerealia*-type pollen are more important from 5200 to 4500 a cal BP during the Early Bronze Age, a period marked by an increase of the population in the South Caucasus (Fig. 7) and the first archeological evidence of agriculture around Gilli wetland (Hovsepyan, 2013, 2017). During this period, the Kura-Araxes culture is present in the South Caucasus and archeological data show the development of permanent village communities and agro-pastoral systems at any elevation in Armenia (Badalyan, 2014).

Then, a maximum of *Cerealia*-type pollen is recorded at 4300 a cal BP followed by a strong decrease from 4100 to 3700 a cal BP. The decline of agricultural practices at Vanevan is consistent with few archeological remains around Gilli wetland and with a decline of the population in the South Caucasus (Hovsepyan, 2013, 2017; Palmisano et al., 2021). However, very little is known about the Middle Bronze Age and archeological sites for this period are scarce. According to Smith (2015), this period is characterized by a shift to more mobile lifeways and not necessarily accompanied by a decline of the population. Our record indicates that agriculture, which was present at the beginning of the Middle Bronze Age on the Sevan shores, became less important around the 4.2 ka climate event, which is characterized by arid conditions around the Mediterranean basin (e.g. Kaniewski et al., 2018; Bini et al., 2019).

From 3600 to 2600 a cal BP (Late Bronze Age, Iron Age I and II), an increase of *Cerealia*-type pollen is recorded and is consistent with the large quantity of archeological sites located on the shores of Lake Sevan and an increase of the population in the South Caucasus (Biscione et al., 2002; Parmegiani and Poscolieri, 2003; Hovsepyan, 2013, 2017; Palmisano et al., 2021). At this period, the Lchashen-Metsamor culture is present around the Lake Sevan and the Urartu empire appears during the Iron Age II. The conception of forts, territory, politics and the development of agriculture, irrigation systems and pastoralism characterized this period (Badalyan et al., 2003).

From 2700 to 2400 a cal BP (Iron Age II and III), a strong decline of *Cerealia*-type pollen is recorded (Fig. 7) probably connected to the end of the Urartu empire and Lchashen-Metsamor culture centered on the north-west of Lake Sevan at 2600 a cal BP (Smith, 2015). At the scale of the Lesser Caucasus, a decline of population seems to occur at around 2700 a cal BP although the data from Palmisiano et al. (2021) are rather incomplete for this period. This period is also marked by the arrival of domination of the Persian Achaemenid Empire in Armenia between 2540 and 2281 a cal BP (Briant, 1996).

From 2300 to 800 a cal BP, *Cerealia*-type pollen strongly increase during the Antiquity and Medieval Period and are consistent with the presence of archeological sites located on the shores of Gilli wetland and Lake Sevan (Parmegiani and Poscolieri, 2003; Hovsepyan, 2013, 2017). *Cerealia* percentages up to 40% suggest crops close or within the wetland. If located in the wetland, a drainage system would have been required in conjunction with fire utilization to suppress semi-aquatic vegetation. At this period, increase of fire activity is recorded in Armenia (Joannin et al., 2014; Cromartie et al., 2020) and Georgia (Connor, 2011). This period is also consistent with the conquest of Alexander the Great in 2281 a cal BP (Briant, 1996) and the foundation of the Kingdom of Armenia, which contributed to a change of human practices.

Pastoralism

Pastoral activities are complex to detect in pollen records (Fig. 7). Similarly to the modern pollen samples, anthropogenic indicators such as *Plantago lanceolata* and *Rumex*-type (Behre, 1981) are present in very low proportion whereas extensive pastoralism existed since the Neolithic in Armenia (Badalyan et al., 2004; Hovsepyan and Willcox, 2008; Badalyan and Harutyunyan, 2014). During the Late Neolithic and the Chalcolithic (7900-6000 a cal BP), the occurrence of *Rumex*-type suggests two phases of grazing (Behre, 1981), corresponding to increases in cereal cultivation and population in the South Caucasus (Fig. 7) and was already observed by Leroyer et al. (2016).

From 4100 to 3700 a cal BP (Middle Bronze Age), no pollen indicators of pastoralism are recorded. At Vanevan, the decline of agriculture is not accompanied by a shift to more mobile lifeways centered on pastoralism as mentioned by Smith (2015). Several studies show a significant impact of the 4.2 ka climate event on Near East societies, hypothesize population decline or migration (Kaniewski et al., 2018; Palmisano et al., 2021). Our data seem to agree for a decline of local population around Lake Sevan.

During the last 3700 a cal BP, pollen of *Plantago lanceolota*, are continuously recorded at Vanevan, although in low percentages. This pollen may be an indicator of pastoralism activities (Behre, 1981). Since the Early Bronze Age (5500 a cal BP), bones of domestic animals are recorded in archaeological materials and confirm the presence of herds of cattle around Gilli wetland (Hovsepyan, 2017). At Zarishat, the last 3000 a cal BP are also marked by a continuous record for *Plantago* and *Rumex*-type (Joannin et al., 2014).

The succession of *Rumex*-type then *Plantago* along the Holocene raises questions about pastoral practices and particularly livestock types for each period (cow, sheep, goat, horse). However, these anthropogenic taxa are also common in mountain steppe environment and it is difficult to unequivocally associate them with specific practices.

5.3 Holocene vegetation dynamics for the Lesser Caucasus

Steppe grassland vegetation with pioneer trees during the Early Holocene (9700-8000 a cal BP)

The Vanevan sequence covers most of the Holocene but does not document the Chenopodiaceae steppe recorded before 10,000 a cal BP when it got replaced by grassland steppes (Wick et al., 2003; Messager et al., 2013; Joannin et al., 2014; Cromartie et al., 2020). From 9700 to 8000 a cal BP, the steppe vegetation is primarily dominated by Poaceae and secondarily by Chenopodiaceae and *Artemisia* (Fig. 7). During this period, open vegetation is also recorded in the Southern Caucasus and the Near East mainly, although the dominant steppic taxa varies from (1) Poaceae (this study; Roberts et al., 2001; Stevens et al., 2001; Wick et al., 2003; Stevens et al., 2006;Ryabogina et al., 2018; Cromartie et al., 2020), to (2) *Artemisia,* (Djamali et al., 2008; Joannin et al., 2014; also in Central Asia: Chen et al., 2008; Zhao et al., 2009, 2020) or (3) Chenopodiaceae (Leroy et al., 2013; Messager et al., 2013). In contrast, the sites north-west of Armenia document forested phases during the same part of the Early Holocene (Connor, 2011; Shumilovskikh et al., 2012; Messager et al., 2017; Connor et al., 2018; Grachev et al., 2020). At Vanevan, a low proportion of arboreal pollen taxa is recorded (Fig. 7). There, the occurrence of *Carpinus betulus*, *Betula* and *Quercus* observed is also recorded at Shenkani (Cromartie et al., 2020), suggesting that these taxa mostly represent regional vegetation. From 9500 to 8500 a cal BP, *Ephedra distachya*-type, *Hippophae,* and *Betula* expand. *Ephedra*, which has a long-distance dispersal by wind (Herzschuh, 2007; Djamali et al., 2009), is indicative of dry climate conditions and is also observed at Lake Van during the Early Holocene (Wick et al., 2003). *Hippophae,* according to the modern relationship between pollen and vegetation, represents the local vegetation bordering Gilli wetland (Fig. 3). *Betula*, which is simultaneously recorded at Shenkani (Cromartie et al., 2020) and Lake Van (Wick et al., 2003), is a pioneer taxon. After this pioneer phase, the arboreal taxon richness increases from 8500 a cal BP with the appearance of several deciduous trees that represent the regional vegetation such as *Carpinus orientalis* and *Carpinus betulus.*

Mixed steppe and open woodlands during a truncated Mid Holocene (8000-5100 a cal BP)

During the Mid Holocene, the vegetation remains steppic but becomes more mixed with Poaceae, *Artemisia*, Chenopodiaceae and Cichorioideae (Fig. 7). From 5900 a cal BP, Poaceae decrease progressively with the same dynamic recorded at Shenkani (Cromartie et al., 2020). The arboreal pollen are dominated by *Quercus* (<10%) and the percentages remain low with a maximum recorded at 7800 a cal BP. Older palynological studies have suggested the presence of deciduous forests on the slopes of Lake Sevan during the Middle Holocene in particular around 6000 years (e.g. Sayadyan et al., 1977; Sayadyan, 1978, 1983; Moreno-Sanchez and Sayadyan, 2005). However, modern pollen-vegetation relationships demonstrated that *Quercus* pollen could represent up to 15% even if no trees were present in the catchment (Fig. 3). More likely, a *Quercus* forest was not present on the slopes of Lake Sevan during the Mid-Holocene. In contrast, *Juniperus* is also well recorded at this period. According to Figure 3, *Juniperus* is mainly an indicator of the local vegetation and could have lived on the slopes such as today where it grows as open woodland. Therefore, the Vanevan's landscape, with nearby grasslands and scarce open woodlands, resembles similar pollen assemblages from Armenia (Joannin et al., 2014; Cromartie et al., 2020) and Iran (Djamali et al., 2008) during the Mid-Holocene. However, Vanevan's pollen record differs by an abrupt drop of arboreal taxa between 6300-5700 a cal BP. The increase of *Artemisia*, Chenopodiaceae, Cichorioideae and *Alchemilla* can be an indicator of both dry climate and pastoralism activities.

Steppe grassland and limited tree diversity (5100-700 a cal BP)

The major vegetation change, initiated at 5400 and which fully settled after 5100 a cal BP, is characterized by an increase of Poaceae, a drop of arboreal taxa (*Quercus, Betula)* and wetland changes (Fig. 7*)*. The decrease of *Betula* is also recorded in Armenia (Cromartie et al., 2020), Turkey (Wick et al., 2003), and at a larger scale in East Asia (Qian et al., 2019). At Vanevan, the vegetation changes around 5100 a cal BP can be discussed in light of the presence of important fires (detected by macro-charcoals) that have affected the landscape and the wetland itself (Leroyer et al., 2016). Several hypotheses explain the ignition of fires: (1) an anthropogenic cause with the lighting of fires by the local population living around Gilli wetland; (2) a volcanic origin due to nearby lava flows from Porak volcano dated to the Mid-Holocene (Fig. 1C, Karakhanian et al., 2017; Meliksetian et al., 2021) or (3) a climatic driver linked with the aridification period around 5000 a cal BP recorded in Armenia (Joannin et al., 2014), Georgia (Connor and Kvadadze, 2008; Connor, 2011), Turkey (Wick et al., 2003), Iran (Stevens et al., 2001, 2006) and in Israel (Bar-Matthews et al., 1997). Although this event could be multifactorial, the regional scale of the changes points towards a climatic cause.

From 4200 to 800 a cal BP, the steppe vegetation continues to dominate the landscape with Poaceae (Fig. 7) in accordance with the Zarishat (Joannin et al., 2014) and Shenkani records (Cromartie et al., 2020). According to the modern pollen-vegetation relationships (Fig. 3), Chenopodiaceae is better recorded in pollen assemblages at low and mid-elevations in Armenia (<1900 m) where the climate conditions are more arid. The increase of Chenopodiaceae between 4400-3500 a cal BP may therefore be an indicator of aridification. A decline of agriculture is also highlighted around 4000 a cal BP and abandoned crops may have favored the expansion of Chenopodiaceae. However, this dynamic is not visible during other agriculture abandonments at Vanevan, therefore the climate appears as the main driver of vegetation change at 4.2 cal yr BP (e.g. Kaniewski et al., 2018; Bini et al., 2019).

5.4 Holocene climate reconstructions for the Lesser Caucasus

5.4.1 Pertinence and reliability of climate reconstructions

Pollen-based climate reconstructions

The results of the four quantitative pollen-based climate reconstructions are consistent (Fig. 5), whether for commonly-used transfer functions/assemblages methods (WAPLS, MAT) or recent “machine-learning” methods (RF, BRT). The minor discrepancies observed in the climate reconstructions at Vanevan can be method-dependent. For the MAT, a major limitation can be the occurrence of no-analogs, however, at Vanevan, it is clearly not the case because the fossil assemblages mainly correspond to the modern Armenian analogs added in this study, as demonstrated by the comparison of modern and core samples (Fig. 4). This method also tends to select analogs that are geographically close to each other (spatial autocorrelation; Telford and Birks, 2005, 2009, 2011), however, at Vanevan the spatial autocorrelation is relatively low (Moran’s I<0.26, p-value<0.01). The MAT shows a high variability among the reconstructed values of close samples, and this variability is linked to the high degree of sensitivity of the method (Brewer et al., 2008) but is probably overestimated for the Holocene period (Fig. 5). The WAPLS performs well and this method is particularly useful for local to regional scale reconstructions (Chevalier et al., 2020); its main disadvantage is the overestimation of the values (Fig. 5) linked to the implicit inverse regression in WAPLS that ‘‘pulls’’ the predicted values toward the mean of the training set (Birks, 1998). The reconstructed values of the RF show low amplitude variations in contrast to the values of other methods. The BRT include the “boosting’ which increases the performance of the model, however the curves present a high sample-to-sample variability. The BRT results are preferred for the regional climate comparison (Fig. 8) since this method is the most performant (maximum R^2 and the minimum RMSE values for all climatic parameters - Supplementary Table S4).

At Vanevan, the pollen-based climate reconstructions are problematic for two periods: (1) between 9700 to 9400 a cal BP, the high temperature and precipitation trends are contradictory to all other climate reconstructions available in the South Caucasus (Fig. 8) and to the brGDGT results, suggesting that this overestimation is probably due to the low pollen taxa diversity and the dominance of Cichorioideae , a very resistant pollen grain (Lebreton et al., 2010); (2) From 2300 a cal BP onwards, the climate trends of the different methods diverge, when the percentages of *Cerealia*-type become important (19-44%). There, it is expected that human activities (agriculture, pastoralism) modified the vegetation structure, composition, and diversity, influencing the paleoclimate reconstructions (St Jacques et al., 2015). Therefore, the pollen-based climate reconstructions for these two periods (9700-9400, and 2300-800 a cal BP) are not considered in the comparison of climate reconstructions and in the climate synthesis (Fig. 8).

BrGDGT temperature reconstructions

At Vanevan, the wetland dynamic changes along the Holocene with a lake system from 9700 a cal BP, a drying phase at 5000 a cal BP and finally the development of a peatland. The type of wetland, the water level and the surrounding vegetation may influence the brGDGT distribution and origins (catchment soils, rivers, in situ production in waters or sediments) (Martin et al., 2019; Martinez-Sosa et al., 2021). The water level and aquatic plant community changes of the wetland may have largely impacted the brGDGT distribution. For example, between 4800 and 3000 a cal BP, the high ΔMAAT is associated with a low water-level and a switch to ferns. The peak of ΔMAAT at 1820 a cal BP is also associated to a change in plant aquatic distribution, Cyperaceae largely decrease whereas *Potamogeton* and *Sparganium/Typha* increase. The local dynamic has therefore largely impacted the brGDGT distribution and could overprint the climate signal. The type of sediment has also impacted the distribution of brGDGTs. The tetramethylated brGDGTs are more abundant in peat sediments whereas the hexamethylated brGDGTs, brGDGTs ΣIIb and brGDGTs ΣIIc are more abundant in lake sediments (Fig. 6BC), confirming the distributions of brGDGTs reported in lakes, peats and soils (Naafs et al., 2018; Russell et al., 2018). Due to the difference in brGDGT distributions and the in-situ production in lakes, if a soil-based MBT-CBT calibration is applied on lake samples, the reconstructed temperatures are generally underestimated (e.g. Sun et al., 2011; Loomis et al., 2011, 2012; Russel et al., 2018).

In the Vanevan core, the difference in the distribution of brGDGTs according to the type of sediment is well identified (Fig. 6C), for this reason a lake calibration was applied from 9700 to 5100 a cal BP whereas a soil calibration was applied from 4900 to 790 a cal BP (Fig. 6D). A soil calibration is applied because the peat samples of Vanevan core are closer to global soils than global peats (Fig. 6B). Moreover, the temperature reconstructed for the surface sample of Vanevan peat is closer to modern temperatures when soil calibration is applied. The ΣIIIa/ΣIIa values suggest important terrigenous sources of brGDGTs in the Vanevan peat (Xiao et al., 2016; Martin et al., 2020).

Global lake calibrations applied to our modern lake samples (Sevan core top and Vanevan surface sample) tend to overestimate the reconstructed temperatures, with values close to warmest month mean (MTWA). The overestimation of reconstructed temperatures has already been evidenced in middle- and high-latitude lakes and could be linked to a seasonal bias (e.g. Foster et al., 2016; Dang et al., 2018; Cao et al., 2020). Both higher brGDGT production during warm seasons (Pearson et al., 2011; Shanahan et al., 2013) or winter ice formation on lake surfaces limiting air/lake water exchanges (Cao et al., 2020) could explain this seasonal bias. To account for the overestimated temperature values in our sequence, they were normalized to their mean values on each part of the record in the following discussion (ΔMAAT, Fig. 6D). The development of local and regional calibrations

Comparison of climate reconstructions based on pollen and brGDGTs (Fig. 8)

The Early Holocene is characterized by cold and dry conditions as indicated by pollen and brGDGT climate reconstructions. The Mid-Holocene (8200-5500 a cal BP) shows warmer conditions associated with a decrease in precipitation by pollen and in temperature by brGDGTs at 6000 a cal BP. Between 5100 and 4800 a cal BP, an important change in wetland dynamic and a drying phase are recorded and have largely impacted the distribution of brGDGTs and the pollen conservation. Therefore, this part will not be considered for climate reconstructions. Then, the climate reconstructions based on pollen and brGDGTs during the last 5000 a cal BP differ because of (1) the change in water level and aquatic plant which impact the bacterial community and therefore the brGDGT distribution and (2) the strong human impact during the last 3000 a cal BP which biased the climate reconstruction based on pollen. However, both climate reconstructions based on pollen and brGDGTs recorded a decrease in temperature between 6300-5700 a cal BP and 4200-3700 a cal BP.

5.4.2 Millennial-scale climate changes in the Lesser Caucasus

A cold and arid Early Holocene (9700-8200 a cal BP)

Vanevan climate reconstructions clearly indicate low annual temperature and precipitation during the Early Holocene (Fig. 8), followed by a rise from 8700 a cal BP. This climate improvement is also accompanied by the increase in water level in Vanevan wetland. This climate pattern is echoed in Armenia and in Georgia: due to time resolution difference between these archives, the climate change goes from more progressive in Georgia (Connor and Kvavadze, 2008) to more abrupt in Armenia (Joannin et al., 2014; Cromartie et al., 2020). In Arid Central Asia, the Early Holocene is also characterized by arid conditions (Chen, et al., 2008). In contrast, in the Near and Middle East (Iran, Turkey and Israel), low values of the oxygen isotopes are generally interpreted as responding to higher water levels, suggesting higher precipitation during the Early Holocene (Roberts et al., 2001; Stevens et al., 2001, 2006; Wick et al., 2003; Bar-Matthews et al., 2003). However, the openness of the vegetation recorded at such a large extent (South Caucasus, Near East, Central Asia) brings into question this climate interpretation. Therefore, our study brings a new argument to attribute cold and dry conditions during the Early Holocene for the whole Near East region. Going into details, several studies in Armenia (Joannin et al., 2014), Iran (Stevens et al., 2001), and Turkey (Wick et al., 2003) attributed the vegetation changes to low spring precipitation, a limiting factor for the plants' growing season, controlled by the Siberian High (Wick et al., 2003). This is not contradictory with the wet Early Holocene identified by isotope data of the Near East if it is the result of high winter precipitation, a parameter typical of the Mediterranean climate (Stevens et al., 2001, 2006; Djamali et al., 2010). Indeed, the winter snows have lower $\delta^{18}O$ values leading to more negative values and a lower total precipitation (Stevens et al., 2001, 2006). Moreover, according to Messager et al. (2017), the winter snow accumulated can melt during spring and summer, generating higher water level in lakes. However, isotopic and lake-level studies are rarely conducted together rendering this interpretation difficult to extrapolate for the Early Holocene. In addition, lake variations depicted in Sevan by our study and Sayadyan's works (1977-1983) do not corroborate a high lake level during the second half of the Early Holocene.

Abrupt installation of warm and humid Mid Holocene progressively shifting to cooler and drier conditions

The Mid Holocene starts with high precipitation and temperature suggested by brGDGTs, pollen and water-level changes (Fig. 8). This agrees well with the warm and humid Mid-Holocene documented in Armenia and Georgia (Connor and Kvavadze, 2008; Joannin et al., 2014; Cromartie et al., 2020), and in Arid Central Asia (Chen et al., 2008). In contrast, the isotopic curves of the Near East show a progressive decrease of precipitation throughout this period (Roberts et al., 2001; Stevens et al., 2001, 2006; Wick et al., 2003; Bar-Matthews et al., 2003). Our study thus records a mid-Holocene climatic optimum and supports an increase of spring precipitation linked to the Westerlies (Wick et al., 2003; Joannin et al., 2014). This change marks the installation of the present-day climate dominated by late spring rainfall over the East Anatolia and North Iran. Since 5100 a cal BP, pollen and low water levels suggest a large decrease in precipitation, while brGDGTs shows a temperature decrease (Fig. 8). This trend agrees with Georgian and Central Asia records for declining precipitation. At the scale of the Near East, our study clarifies the climate pattern with conditions becoming colder, and aridification (Roberts et al., 2001; Stevens et al., 2001, 2006; Wick et al., 2003; Bar-Matthews et al., 2003). Since this period, humans were able to live and cultivate nearer Gilli wetland thanks to the water level drop.

5.4.3 Rapid/abrupt climate events in the Lesser Caucasus

6.2 and 5.2 ka arid events

At Vanevan, the Mid-Holocene is marked by two arid events. The first one is recorded at 6300-5700 a cal BP and appears both in pollen and brGDGT reconstructions (Fig. 8). In the South Caucasus, the fire frequence history and abundance variations of sedge at Zarishat in Armenia show a drier phase at 6400 a cal BP (Joannin et al., 2014). At a larger scale, a drop in rainfall occurs at Lake Zeribar (Iran) at 6200 a cal BP (Stevens et al., 2006), at Sofular cave (Turkey) at 6200-6000 a cal BP (Zanchetta et al., 2014) and in East Asia at 6.2 ka, linked to an abrupt monsoon event (Yu et al., 2006; Wu et al., 2018). Considering temperature, there is no clear trends according to our results (Fig. 8) and the other studies carried out in the South Caucasus and the Near East.

The second arid event recorded at Vanevan occurs at 5100-4800 a cal BP and is marked by a drop in arboreal trees, a drying wetland phase, high fire activity, and changes in brGDGT distribution (Fig. 8). Major changes are also recorded in Armenia: at Zarishat, by fire frequence history and sedge changes, which show a dry phase at 5300-4900 a cal BP (Joannin et al., 2014); at Shenkani, by an increase of fire activity for the same period (Cromartie et al., 2020); and in Georgia at Lake Aligol, by an increase of fires accompanied by a drop in rainfall at 5000-4500 a cal BP (Connor and Kvavadze, 2008). In the Caucasus, glacier advances are recorded at 5000-4500 a cal BP, supporting the hypothesis of a colder climate in the Caucasus (Solomina et al., 2015). In the Near East, an arid phase is visible in isotopic data at Lake Mirabad and Zeribar in Iran at 5200 a cal BP (Stevens et al., 2001, 2006), at Gölhisar in Turkey at 4900 a cal BP (Eastwood et al., 2007) and at Soreq cave in Israël at 5200 a cal BP (Bar-Matthews et al., 1997; Bar-Matthews and Ayalon, 2011). Magny et al. (2006) define the '5.2 ka event' as a global climate event, characterized by drier conditions around the Mediterranean basin. Although agriculture practices are present around Gilli wetland since 5200 a cal BP, the changes of vegetation and fire between 5300 and 4800 a cal BP are regional and seem to be largely affected by the aridification event.

The 4.2 ka arid event

At Vanevan, a period of aridity between 4200 and 3700 a cal BP is recorded by the pollen climate reconstruction, water-level, and brGDGT changes. This event is characterized by a drop in annual and summer precipitation and an increase in summer temperature. The brGDGT reconstructions confirm warm conditions for this period (Fig. 8). In the South Caucasus, the other pollen sequences do not clearly record this arid event, except at Shenkani where an increase of the Br/Ti ratio indicates a decrease in terrigenous inputs between 4300 and 4100 a cal BP (Cromartie et al., 2020). In the Near East, the isotopic data of Lake Zeribar in Iran (Stevens et al., 2001), Eski Acigöl in Turkey and Soreq cave in Israel (Bar-Matthews et al., 2003) show a climate aridification around 4000 a cal BP. At Lake Van in Turkey, arid conditions at 4200-4000 a cal BP are expressed through the increase of fire, the decrease of *Quercus* and low lake-level (Wick et al., 2003). This arid event is also characterized by an increase of dust deposits in the Near East (Ön et al., 2021) as at Lake Van in Turkey (Lemcke and Sturm 1997) and at Lake Neor in Iran (Sharifi et al., 2015). However, this dust event is not recorded in the South Caucasus (Cromartie et al., 2020). The 4.2 ka event is defined by a severe and prolonged drought around the Mediterranean basin (global "megadrought", Weiss, 2016). It was first proposed by Weiss et al. (1993) for the Near East and is recorded at a global scale although not evidenced in all records (Cullen et al., 2000). The 4.2 ka event is today considered as the formal boundary of Late and Middle Holocene. This event is often characterized as a cold event (Cullen et al., 2000; Dixit et al., 2014), however for the Eastern Mediterranean the records show warmer conditions (this study; Bini et al., 2019). In this region, the 4.2 ka event is defined by climatic and environmental changes that extend between 4.3 and 3.8 ka (Bini et al., 2019). In the South Caucasus, the Vanevan sequence is the first to report the impact of a warm and arid 4.2 ka event. The concordance between the 4.2 ka event and the decline of agricultural practices is easily linkable to the decline of local population but cannot tell whether it is due to societal collapse or migrations of population in the South Caucasus and the Near East (Kaniewski et al., 2018; Palmisano et al., 2021).

The 2.8 ka climate event

Between 2900 and 2400 a cal BP, a cold and arid event appears at Vanevan, mainly with the WAPLS method (Fig. 8). This pattern is consistent with the glacier advances recorded in the Greater Caucasus at 2900-2800 a cal BP (Solomina et al., 2015) and the drop in rainfall at Lake Van, in Turkey (Wick et al., 2003) and Soreq Cave, in Israël (Bar-Matthews et al., 2003). The 2.8 ka event is defined by cold conditions at a global scale and several studies have also identified its impact in East Asia (Fukumoto et al., 2012) and Europe (Ivy-Ochs et al., 2009; Van Geel et al., 2014). In the South Caucasus, our climate reconstructions marked the impact of the 2.8 ka event, which is accompanied by a decline of agricultural practices around Lake Sevan, certainly due to a decline of local population (Fig. 8). This climate event may have contributed to the decline of the Urartian empire centered around Lake Sevan and it coincides with the arrival of the Persians in Armenia. At the scale of the Caucasus, Palmisiano et al. (2021) also showed a decline of population at 2700 a cal BP although the data are limited for this period. According to several studies focused on the Near East, the demographic trends become dissociated from climate from 4000-3500 a cal BP because populations are more resilient due to the technological advancement (Lawrence et al., 2016; Roberts et al., 2019). This hypothesis might need to be revisited in the light of the present study, at least for the South Caucasus.

Atmospheric processes

The abrupt climate events described here are all characterized by arid conditions in the Caucasus and the Near East. Temperature shows colder conditions for the 5.2 ka and 2.8 ka events whereas the 4.2 ka event is characterized by warmer conditions. Several studies indicate that the North Atlantic Oscillation (NAO) is the main driver of precipitation variability in the Near East and the Caucasus during the Mid- and Late Holocene (Joannin et al., 2014; Jones et al., 2019). Therefore, arid events in the Eastern Mediterranean can be caused by a weak westerly flow associated to multi-centennial cyclicity of the NAO system (e.g. Magny et al., 2013; Zielhofer et al., 2017; Bini et al., 2019). Many studies suggest that the Westerlies decreasing influence is accompanied by the reinforcement and latitudinal expansion of the Siberian High and subtropical systems (Djamali et al., 2008; Joannin et al., 2014; Zanchetta et al., 2016; Bini et al., 2019; Ön et al., 2021). The southward expansion of the Siberian High provides the incursion of cold-dry air masses in southern Europe (Zanchetta et al., 2016; Perşoiu et al., 2019). We hypothesize that the 5.2 ka and 2.8 ka events are mainly under the influence of the winter Siberian High as cold conditions are recorded in the South Caucasus and the Near East. According to Perşoiu et al. (2019), the 4.2 ka event is also characterized by a dominance of the winter Siberian High in Europe, however, the records of the South Caucasus and the Near East show warm conditions (this study; Bini et al., 2019). Other atmospheric systems could come into play in these regions during the 4.2 ka event. According to Ön et al. (2021), precipitation of the southeastern Mediterranean is mainly controlled by the latitudinal migration of the Intertropical Convergence Zone and the subtropical high pressure belt but the model does not specify clear trends on the aridity or temperature in the Near East. Noteworthy, the study of Sharifi et al. (2015) evidences the arrival of dust from the Middle East coming from the south, but does not identify the origins. We hypothesize that the 4.2 ka event in the South Caucasus and the Near East is influenced by the northward migration of subtropical systems providing warm and arid conditions. This migration is also reflected through the arrival of dust from the Near East but not reaching the South Caucasus. Considering the 6.2 ka event, it is also linked to the NAO variations (Joannin et al., 2014), however, the contradicting temperature reconstructions from Vanevan do not allow us to hypothesize whether the 6.2 ka arid event is due to polar or Arabian subtropical influences.

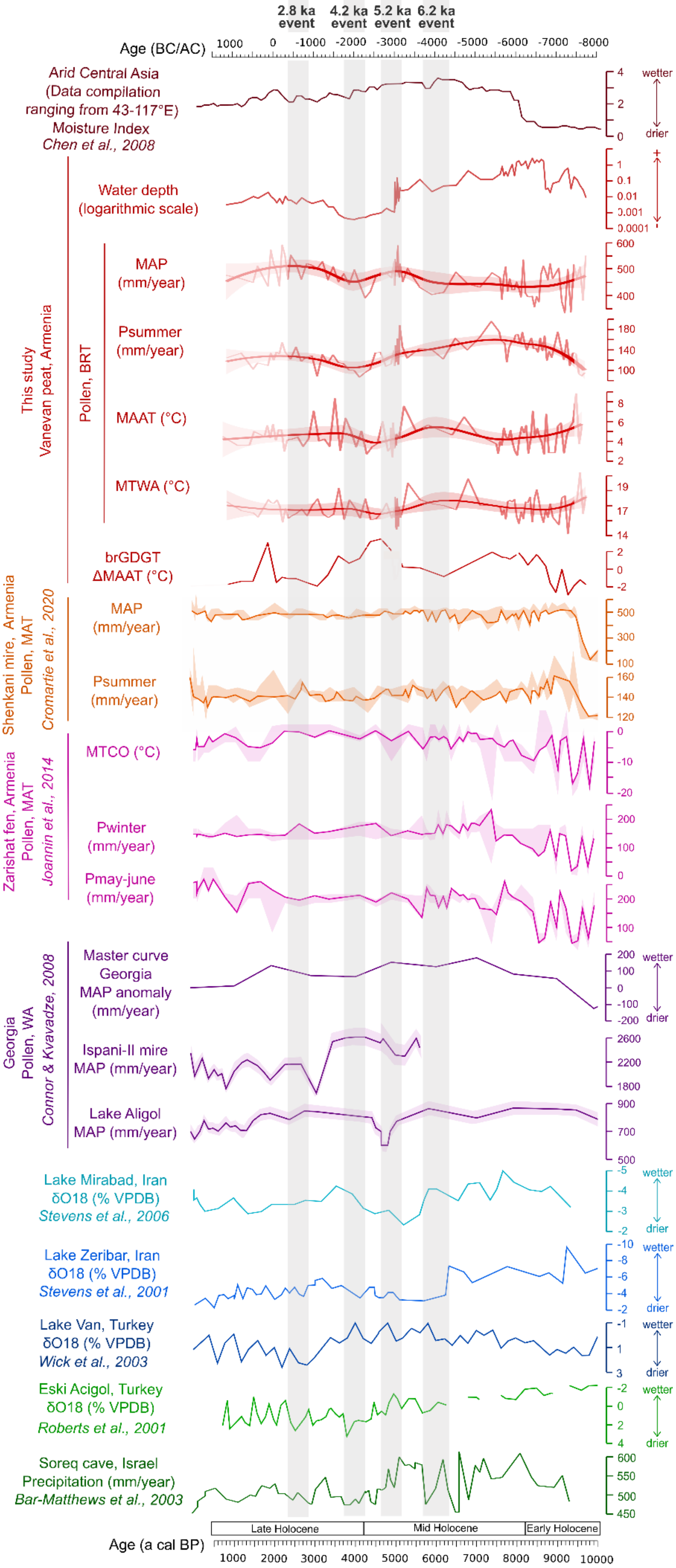

2.8 ka event
4.2 ka event
5.2 ka event
6.2 ka event
Age (BC/AC)
Arid Central Asia (Data compilation ranging from 43-117°E) Moisture Index
Chen et al., 2008
wetter
drier
Water depth (logarithmic scale)
MAP (mm/year)
Psummer (mm/year)
MAAT (°C)
MTWA (°C)
This study Vanevan peat, Armenia
Pollen, BRT
brGDGT ΔMAAT (°C)
Shenkani mire, Armenia Pollen, MAT Cromartie et al., 2020
MAP (mm/year)
Psummer (mm/year)
Zarishat fen, Armenia Pollen, MAT Joannin et al., 2014
MTCO (°C)
Pwinter (mm/year)
Pmay-june (mm/year)
Georgia Pollen, WA Connor & Kvavadze, 2008
Master curve Georgia MAP anomaly (mm/year)
Ispani-II mire MAP (mm/year)
Lake Aligol MAP (mm/year)
Lake Mirabad, Iran δO18 (% VPDB) Stevens et al., 2006
Lake Zeribar, Iran δO18 (% VPDB) Stevens et al., 2001
Lake Van, Turkey δO18 (% VPDB) Wick et al., 2003
Eski Acigol, Turkey δO18 (% VPDB) Roberts et al., 2001
Soreq cave, Israel Precipitation (mm/year) Bar-Matthews et al., 2003
Late Holocene
Mid Holocene
Early Holocene
Age (a cal BP)

1173

Figure 8. Synthesis of paleoenvironmental records over the last 10,000 yrs based on pollen, brGDGTs and $\delta^{18}O$ data. Gray vertical shading represents abrupt climate events. MAAT: mean annual air temperature. MTWA: mean temperature of the warmest month. MAP: mean annual precipitation. Psummer: summer precipitation. For location, refer to Fig. 1.

6. Conclusions

Environmental dynamic, climate changes and human practices are reconstructed using multi-proxies at Vanevan peat in Armenia during the last 9700 years. This study extends the Mid-Holocene record documented at Vanevan peat by Leroyer et al. (2016) and proposes new proxies as brGDGTs.

- For the first time in the South Caucasus and the Near East, our study provides climate reconstructions based on brGDGTs and pollen coupled with a multimethod approach (MAT, WAPLS, RF, BRT). The climate reconstructions are complementary and show a good correspondence between the proxies and the methods used. However, our results reveal that it is essential to understand the local dynamic of the wetland to properly interpret the climate reconstructions based on brGDGTs and pollen. The results show an arid and cold Early Holocene, a more humid and warmer Mid Holocene, and a more arid and cooler Late Holocene. Several abrupt events are detected at 6.2 ka, 5.2 ka, 4.2 ka, 2.8 ka and allow us to highlight the atmospheric processes in the Caucasus and the Near East. The four climate events are arid and seem linked to weak westerlies associated to multi-centennial cyclicity (NAO-like). The 5.2 ka and 2.8 ka are characterized by cold conditions and could be associated to a strong Siberian High. On the contrary, the 4.2 ka is characterized by warm conditions and would be influenced by the northward migration of Arabian subtropical systems.
- This study is also the first to investigate the modern relationship between vegetation and pollen in Armenia. It complements the study of Connor and Kvavadze (2008) for Georgia. The results show an abundance of Chenopodiaceae in semi-desert/steppe regions and Poaceae in steppes, subalpine and alpine meadows. Chenopodiaceae and *Artemisia* are over-represented whereas Poaceae is reliably associated with the local vegetation. In the South Caucasus, Chenopodiaceae percentages seem to be a better aridity index than A/C ratio.
- The vegetation during the last 9700 years shows a dominance of steppes predominantly composed of Poaceae. The surrounding vegetation of Lake Sevan was poorly forested, even during the Mid-Holocene and contrasts with the previous hypotheses which suggested the occurrence of a deciduous forest. This result brings into question the existence of open woodland around Lake Sevan and new studies are necessary to better estimate the vegetation around the entire lake and the relationship to open woodland.
- Humans have been able to live and cultivate when the Gilli wetland level dropped at around 5200 a cal BP. The expansion and decline phases of agricultural practices are remarkably correlated with the occupation and abandonment phases of archeological sites of Lake Sevan but also with demographic trends of the South Caucasus (Palmisano et al., 2021).

- Major changes in paleohydrological conditions are recorded by abundances of aquatic plants and algae at Vanevan during the last 9700 a cal BP. A lake system is initially present following by a drying phase at 4950 a cal BP associated with fire and finally a peatland dominated by Cyperaceae appears. The water level changes are consistent with the previously established variations of Lake Sevan in Sayadyan's works (1977-1983) and they are congruent with our climate reconstructions proposed for the South Caucasus.
- Contrary to several studies, which conclude to the dissociation between demographic trends and climate from 4000-3500 a cal BP in the Near East, our study suggests a significant impact of abrupt climate changes on populations. The different events are consistent with the population abandonment phases and question the human enfranchisement in the face of climate changes due to their technological advancements. In our study, climate changes appear as one of the main drivers of vegetation and demographic changes in the South Caucasus. However, further research is needed to understand all the social complexities related to these changes although our study clearly shows links between climatic changes and demographic shifts.

In the line with the previous studies of Joannin et al. (2014), Leroyer et al. (2016) and Cromartie et al. (2020) for Armenia, this new study brings a better understanding of vegetation dynamics and the respective role of climate and humans in the South Caucasus. The multiproxy approach provided a robust chronicle of climate changes occurring during the Holocene.

Funding

This research was co-founded by the International PhD course in "Agriculture Technologies and Biotechnologies" (34° Cycle, Code: DOT1339335). Financial support for this study was provided by the French–Armenian International Associated Laboratory HEMHA "Humans and Environments in Mountainous Habitats, the case of Armenia" supervised by C. Chataigner and P. Avetisyan. This programme between Armenia and France was founded by the French National Centre for Scientific Research (CNRS). Field trip campaigns and analyses were founded by CNRS program INSU INTERRVIE (PI: C. Colombié) and Labex OT Med and ECCOREV program from Aix-Marseille University through the GeoArT and SoCCER project (PI: V. Ollivier). For the analytical work completed at LGLTPE-ENS de Lyon, this research was funded by Institut Universitaire de France funds to G. Ménot. The travels between Italy and France were financed by VINCI founding. The conference funding was provided by the Association des Palynologues de Langue Française (APLF).

Author contributions

M. Robles: Conceptualization, Field work, Laboratory work, Formal analysis, Writing draft manuscript, Review, Funding acquisition. S. Joannin: Project administration, Conceptualization, Field work, Supervision, Review, Funding acquisition; O. Peyron: Conceptualization, Formal analysis, Supervision, Review, Funding acquisition. G. Ménot: Conceptualization, Supervision, Review, Funding acquisition; E. Brugiapaglia: Conceptualization, Supervision, Review. L. Dugerdil: Formal analysis, Review. V. Ollivier: Field work, Review, Funding acquisition. S. Ansanay-Alex and A.-L. Develle: Laboratory work. P. Tozalakyan and K. Sahakyan: Field work. K. Meliksetian and L. Sahakyan: Field supervision. R. Badalyan and B. Perello: Field supervision, Review. C. Colombié: Field work, Review, Funding acquisition.

Declaration of competing interest

The authors declare that they have no known competing financial interests or personal relationships that could have appeared to influence the work reported in this paper.

Acknowledgements

The authors would like to express their appreciation to David Etienne for the NPP identification help, to Laurent Bouby and Isabelle Figueiral for seed or wood identifications used for radiocarbon datings, and to Sandrine Canal for the preparation of moss samples. We would like to thank Amy Cromartie for the proofreading and comments on the manuscript.

References

Alekin, O., Ulyanova, D., 1986. Super-saturation of Sevan water with CaC03. Water Resources Moscow I, 117-122 (in Russian).

Arimura, M., Gasparyan, B., Chataigner, C., 2012. Prehistoric sites in Northwest Armenia: Kmlo-2 and Tsaghkahovit, in: Matthews, R.J., Curtis, J. (Eds.), Proceedings of the 7th International Congress of the Archaeology of the Ancient Near East. Volume 3: Fieldwork and Recent Research e Posters. Harrasowitz, Wiesbaden, pp. 135-150.

Arnaud, F., Révillon, S., Debret, M., Revel, M., Chapron, E., Jacob, J., Giguet-Covex, C., Poulenard, J., Magny, M., 2012. Lake Bourget regional erosion patterns reconstruction reveals Holocene NW European Alps soil evolution and paleohydrology. Quaternary Science Reviews 51, 81–92. https://doi.org/10.1016/j.quascirev.2012.07.025

Badalyan, R.S., Smith A.T., Avetisyan P.S., 2003. The Emergence of Socio-Political Complexity in Southern Caucasia: An Interim Report on the Research of Project ArAGATS, in: Smith, A.T. and Rubinson K.S. (Eds.), Archaeology in the Borderlands: Investigations in Caucasia and Beyond. The Cotsen Institute of Archaeology, Los Angeles, pp. 144-166.

Badalyan, R., Lombard, P., Chataigner, C., Avetisyan, P., 2004. The Neolithic and Chalcolithic phases in the Ararat Plain (Armenia): The view from Aratashen, in: Sagona, A. (Eds.), A View from the Highlands-Archaeological Studies in Honour of Charles Burney. Ancient Near Eastern Studies Supplement 12, Peteers, pp. 399-420.

Badalyan, R.S., 2014. New data on the periodization and chronology of the Kura-Araxes culture in Armenia. Paléorient 40, 71–92. https://doi.org/10.3406/paleo.2014.5636

Badalyan, R., Harutyunyan, A., 2014. Aknashen-the Late Neolithic Settlement of the Ararat Valley: Main Results and Prospects for the Research, in: Gasparyan, B., Arimura, M. (Eds.), Stone age of Armenia. Kanazawa University, Kanazawa, pp. 161-177.

Baghdasaryan, A.B., 1958. Klimat Armyanskoy, SSR, Yerevan, pp. 108-118.

Bar-Matthews, M., Ayalon, A. and Kauffman, A., 1997. Late Quaternary paleoclimate in the eastern Mediterranean region from stable isotope analysis of speleothems at Soreq Cave, Israel. Quaternary Res. 47, 155–168. https://doi.org/10.1006/qres.1997.1883

Bar-Matthews, M., Ayalon, A., Gilmour, M., Matthews, A., Hawkesworth, C.J., 2003. Sea–land oxygen isotopic relationships from planktonic foraminifera and speleothems in the Eastern Mediterranean region and their implication for paleorainfall during interglacial intervals. Geochimica et Cosmochimica Acta 67, 3181–3199. https://doi.org/10.1016/S0016-7037(02)01031-1

Bar-Matthews, M., Ayalon, A., 2011. Mid-Holocene climate variations revealed by high-resolution speleothem records from Soreq Cave, Israel and their correlation with cultural changes. The Holocene 21, 163–171. https://doi.org/10.1177/0959683610384165

Behre, K.E., 1981. The interpretation of anthropogenic indicators in pollen diagrams. Pollen et spores, 23(2), 225-245.

Beug, H.-J, 2004. Leitfaden der Pollenbestimmung fur Mitteleuropa und angrenzende Gebeite, Pfeil, Munchen.

Bini, M., Zanchetta, G., Perşoiu, A., Cartier, R., Català, A., Cacho, I., Dean, J.R., Di Rita, F., Drysdale, R.N., Finnè, M., Isola, I., Jalali, B., Lirer, F., Magri, D., Masi, A., Marks, L., Mercuri, A.M., Peyron, O., Sadori, L., Sicre, M.-A., Welc, F., Zielhofer, C., Brisset, E., 2019. The 4.2 ka BP Event in the Mediterranean region: an overview. Clim. Past 15, 555–577. https://doi.org/10.5194/cp-15-555-2019

Birks, H.J.B., 1998. Numerical tools in palaeolimnology-progress, potentialities, and problems. J. Paleolimnol. 20, 307–332.

Biscione, R., Hmayakyan, S., Parmegiani, N., 2002. The North-Eastern frontier: Urartians and Non-Urartians in the Sevan Lake Basin, The Southern Shores. CNR istituto di studi sulle civilt`a dell'Egeo e del Vicino Oriente, Rome.

Blaauw, M., 2010. Methods and code for "classical" age-modelling of radiocarbon sequences. Quat. Geochronol. 5, 512–518. https://doi.org/10.1016/j.quageo.2010.01.002

Blaauw, M., Christen, J.A., 2011. Flexible paleoclimate age-depth models using an autoregressive gamma process. Bayesian analysis 6, 457–474. https://doi.org/10.1214/11-BA618

Bohn, U., Gollub, G., Hettwer, C., 2000. Karte der natürlichen Vegetation Europas, Bundesamt für Naturschutz, Bonn.

Bottema, S., 1992. Prehistoric cereal gathering and farming in the Near East: the pollen evidence. Rev. Palaeobot. Palynol. 73, 21–33.

Braun-Blanquet, J., Schoenichen, W. 1964.Grundzüge der Vege-tationskunde, Springer, Vienna.

Breiman, L., 2001. Random forests. Machine learning 45, 5–32.

Brewer, S., Guiot, J., Sánchez-Goñi, M.F., Klotz, S., 2008. The climate in Europe during the Eemian: a multi-method approach using pollen data. Quaternary Science Reviews, 27, 2303-315. https://doi.org/10.1016/j.quascirev.2008.08.029

Briant, P., 1996. Histoire de l'Empire perse de Cyrus à Alexandre. Fayard, Paris, 1247p.

Brown, E., Johnson, T., Scholz, C., Cohen, A., King, J., 2007. Abrupt change in tropical African climate linked to the bipolar seesaw over the past 55,000 years. Geophys. Res. Lett., 34, L20702. https://doi.org/10.1029/2007GL031240

Cao, X., Tian, F., Xu, Q.H., Li, Y.C., Zhang, Z.Q., Jia, H.J., Zhang, L.Y., Wang, X., 2007. Pollen influx and comparison with surface pollen in the east part of Yinshan Mountains. Acta Palaeontologica Sinica, 46(4), 418 (in Chinese).

Cao, J., Rao, Z., Shi, F., Jia, G., 2020. Ice formation on lake surfaces in winter causes warm-season bias of lacustrine brGDGT temperature estimates. Biogeosciences 17, 2521–2536. https://doi.org/10.5194/bg-17-2521-2020

Chataigner, C., Gratuze, B., 2014. New data on the exploitation of obsidian in the Southern Caucasus (Armenia, Georgia) and eastern Turkey, Part 2: obsidian procurement from the Upper Palaeolithic to the Late Bronze Age. Archaeometry 56 (2), 569-577. https://doi.org/10.1111/arcm.12007

Chataigner, C., Gratuze, B., Tardy, N., Abbès, F., Kalantaryan, I., Hovsepyan, R., Chahoud, J., Perello, B., 2020. Diachronic variability in obsidian procurement patterns and the role of the cave-sheepfold of Getahovit-2 (NE Armenia) during the Chalcolithic period. Quaternary International 550, 1–19. https://doi.org/10.1016/j.quaint.2020.02.010

Chen, F., Yu, Z., Yang, M., Ito, E., Wang, S., Madsen, D.B., Huang, X., Zhao, Y., Sato, T., John B. Birks, H., Boomer, I., Chen, J., An, C., Wünnemann, B., 2008. Holocene moisture evolution in arid central Asia and its out-of-phase relationship with Asian monsoon history. Quat. Sci. Rev. 27, 351–364. https://doi.org/10.1016/j.quascirev.2007.10.017

Chevalier, M., Davis, B.A.S., Heiri, O., Seppä, H., Chase, B.M., Gajewski, K., Lacourse, T., Telford, R.J., Finsinger, W., Guiot, J., Kühl, N., Maezumi, S.Y., Tipton, J.R., Carter, V.A., Brussel, T., Phelps, L.N., Dawson, A., Zanon, M., Vallé, F., Nolan, C., Mauri, A., de Vernal, A., Izumi, K., Holmström, L., Marsicek, J., Goring, S., Sommer, P.S., Chaput, M., Kupriyanov, D., 2020. Pollen-based climate reconstruction techniques for late Quaternary studies. Earth-Science Reviews 210, 103384. https://doi.org/10.1016/j.earscirev.2020.103384

Cohen, A.S., 2003. Paleolimnology: the history and evolution of lake systems. Oxford University Press, New York, 528p.

Connor, S.E., Thomas, I., Kvavadze, E.V., Arabuli, G.J., Avakov, G.S., Sagona, A., 2004. A survey of modern pollen and vegetation along an altitudinal transect in southern Georgia, Caucasus region. Review of Palaeobotany and Palynology 129, 229–250. https://doi.org/10.1016/j.revpalbo.2004.02.003

Connor, S.E., Kvavadze, E.V., 2008. Modelling late Quaternary changes in plant distribution, vegetation and climate using pollen data from Georgia, Caucasus. Journal of Biogeography 36, 529–545. https://doi.org/10.1111/j.1365-2699.2008.02019.x

Connor, S.E., 2011. A promethean legacy: late quaternary vegetation history of southern Georgia, the Caucasus. Peeters, Leuven.

Connor, S.E., Colombaroli, D., Confortini, F., Gobet, E., Ilyashuk, B.P., Ilyashuk, E.A., van Leeuwen, J.F.N., Lamentowicz, M., van der Knaap, W.O., Malysheva, E., Marchetto, A., Margalitadze, N., Mazei, Y., Mitchell, E.A.D., Payne, R.J., Ammann, B., 2018. Long-term population dynamics: Theory and reality in a peatland ecosystem. J. Ecol. 106, 333–346. https://doi.org/10.1111/1365-2745.12865

Cromartie, A., Blanchet, C., Barhoumi, C., Messager, E., Peyron, O., Ollivier, V., Sabatier, P., Etienne, D., Karakhanyan, A., Khatchadourian, L., Smith, A.T., Badalyan, R., Perello, B., Lindsay, I., Joannin, S., 2020. The vegetation, climate, and fire history of a mountain steppe: A Holocene reconstruction from the South Caucasus, Shenkani, Armenia. Quat. Sci. Rev. 246, 106485. https://doi.org/10.1016/j.quascirev.2020.106485

Croudace, I.W., Rothwell, R.G., 2015. Micro-XRF Studies of Sediment Cores: Applications of a Non-destructive Tool for the Environmental Sciences. Springer, Dordrecht.

Cullen, H.M., deMenocal, P.B., Hemming, S., Hemming, G., Brown, F.H., Guilderson, T., Sirocko, F., 2000. Climate change and the collapse of the Akkadian empire: Evidence from the deep sea. Geology 28, 379–382. https://doi.org/10.1130/0091-7613

Dang, X., Ding, W., Yang, H., Pancost, R.D., Naafs, B.D.A., Xue, J., Lin, X., Lu, J., Xie, S., 2018. Different temperature dependence of the bacterial brGDGT isomers in 35 Chinese lake sediments compared to that in soils. Organic Geochemistry 119, 72–79. https://doi.org/10.1016/j.orggeochem.2018.02.008

Davtian, N., Bard, E., Ménot, G., Fagault, Y., 2018. The importance of mass accuracy in selected ion monitoring analysis of branched and isoprenoid tetraethers. Org. Geochem. 118, 58–62. https://doi.org/10.1016/j.orggeochem.2018.01.007

Dearing Crampton-Flood, E., Tierney, J.E., Peterse, F., Kirkels, F.M.S.A., Sinninghe Damsté, J.S., 2020. BayMBT: A Bayesian calibration model for branched glycerol dialkyl glycerol tetraethers in soils and peats. Geochimica et Cosmochimica Acta 268, 142–159. https://doi.org/10.1016/j.gca.2019.09.043

De'ath, G., 2007. Boosted trees for ecological modeling and prediction. Ecology 88, 243-251. https://doi.org/10.1890/0012-9658(2007)88[243:BTFEMA]2.0.CO;2

De Jonge, C., Hopmans, E.C., Zell, C.I., Kim, J.-H., Schouten, S., Sinninghe Damsté, J.S., 2014. Occurrence and abundance of 6-methyl branched glycerol dialkyl glycerol tetraethers in soils: implications for palaeoclimate reconstruction. Geochem. Cosmochim. Acta 141, 97–112. https://doi.org/10.1016/j.gca.2014.06.013

Ding, S., Schwab, V.F., Ueberschaar, N., Roth, V.-N., Lange, M., Xu, Y., Gleixner, G., Pohnert, G., 2016. Identification of novel 7-methyl and cyclopentanyl branched glycerol dialkyl glycerol tetraethers in lake sediments. Org. Geochem. 102, 52–58. https://doi.org/10.1016/j.orggeochem.2016.09.009

Dixit, Y., Hodell, D.A., Petrie, C.A., 2014. Abrupt weakening of the summer monsoon in northwest India ~4100 yr ago. Geology 42, 339–342. https://doi.org/10.1130/G35236.1

Djamali, M., de Beaulieu, J.-L., Shah-hosseini, M., Andrieu-Ponel, V., Ponel, P., Amini, A., Akhani, H., Leroy, S.A.G., Stevens, L., Lahijani, H., Brewer, S., 2008. A late Pleistocene long pollen record from Lake Urmia, Nw Iran. Quat. res. 69, 413–420. https://doi.org/10.1016/j.yqres.2008.03.004

Djamali, M., de Beaulieu, J.-L., Campagne, P., Andrieu-Ponel, V., Ponel, P., Leroy, S.A.G., Akhani, H., 2009. Modern pollen rain–vegetation relationships along a forest–steppe transect in the Golestan National Park, NE Iran. Review of Palaeobotany and Palynology 153, 272–281. https://doi.org/10.1016/j.revpalbo.2008.08.005

Djamali, M., Akhani, H., Andrieu-Ponel, V., Braconnot, P., Brewer, S., de Beaulieu, J.-L., Fleitmann, D., Fleury, J., Gasse, F., Guibal, F., Jackson, S.T., Lézine, A.-M., Médail, F., Ponel, P., Roberts, N., Stevens, L., 2010. Indian Summer Monsoon variations could have affected the early-Holocene woodland expansion in the Near East. The Holocene 20, 813–820. https://doi.org/10.1177/0959683610362813

Djamali, M., Cilleros, K., 2020. Statistically significant minimum pollen count in Quaternary pollen analysis; the case of pollen-rich lake sediments. Rev. Palaeobot. Palynol., 275, 104156. https://doi.org/10.1016/j.revpalbo.2019.104156

Dugerdil, L., Joannin, S., Peyron, O., Jouffroy-Bapicot, I., Vannière, B., Bazartseren, B., Unkelbach, J., Behling, H., Ménot, G., 2021. Climate reconstructions based on GDGT and pollen surface datasets from Mongolia and Siberia: calibrations and applicability to extremely cold-dry environments over the Late Holocene. Climate of the Past Discussions, pp.1-39. https://doi.org/10.5194/cp-2020-154

Eastwood, W.J., Leng, M.J., Roberts, N., Davis, B., 2007. Holocene climate change in the eastern Mediterranean region: a comparison of stable isotope and pollen data from Lake Gölhisar, southwest Turkey. J. Quaternary Sci. 22, 327–341. https://doi.org/10.1002/jqs.1062

El-Moslimany, A., 1990. Ecological significance of common non-arboreal pollen: examples from drylands of the Middle East. Review of Palaeobotany and Palynology 69, 343-350.

Elith, J., Leathwick, J.R., Hastie, T., 2008. A working guide to boosted regression trees. J. Anim. Ecol. 77, 802-813

Fægri, K., Iversen, J., Kaland, P.E., Krzywinski, K., 1989. Textbook of pollen analysis, IV, John Wiley & Sons, Chichester.

Fayvush, G., Tamanyan, K., Kalashyan, M., Vitek, E., 2013. Biodiversity Hotspots in Armenia. Annalen des Naturhistorischen Museums Wien B 115, 11–20.

Fayvush, G., Aleksanyan, A., Bussmann, R.W., 2017. Ethnobotany of the Caucasus – Armenia, in: Bussmann, R.W. (Eds.), Ethnobotany of the Caucasus, European Ethnobotany. Springer International Publishing, Cham, pp. 21–36. https://doi.org/10.1007/978-3-319-49412-8_18

Fick, S.E., Hijmans, R.J., 2017. Worldclim 2: new 1-km spatial resolution climate surfaces for global land areas: New climate surfaces for global land areas. International Journal of Climatology 37, 4302–4315. https://doi.org/10.1002/joc.5086

Fletcher, W.J., Debret, M., Goñi, M.F.S., 2013. Mid-Holocene emergence of a low-frequency millennial oscillation in western Mediterranean climate: Implications for past dynamics of the North Atlantic atmospheric westerlies. The Holocene 23, 153–166. https://doi.org/10.1177/0959683612460783

Foster, L.C., Pearson, E.J., Juggins, S., Hodgson, D.A., Saunders, K.M., Verleyen, E., Roberts, S.J., 2016. Development of a regional glycerol dialkyl glycerol tetraether (GDGT)–temperature calibration for Antarctic and sub-Antarctic lakes. Earth and Planetary Science Letters 433, 370–379. https://doi.org/10.1016/j.epsl.2015.11.018

Fukumoto, Y., Kashima, K., Orkhonselenge, A., Ganzorig, U., 2012. Holocene environmental changes in northern Mongolia inferred from diatom and pollen records of peat sediment. Quaternary International 254, 83–91. https://doi.org/10.1016/j.quaint.2011.10.014

Ge, Y., Li, Y., Bunting, M.J., Li, B., Li, Z., Wang, J., 2017. Relation between modern pollen rain, vegetation and climate in northern China: Implications for quantitative vegetation reconstruction in a steppe environment. Science of The Total Environment 586, 25–41. https://doi.org/10.1016/j.scitotenv.2017.02.027

Göktürk, O.M., 2011. Climate on the southern Black Sea coast during the Holocene: implications from the Sofular Cave record. Quaternary Science Reviews 30, 2433-2445. https://doi.org/10.1016/j.quascirev.2011.05.007

Grachev, A.M., Novenko, E.Y., Grabenko, E.A., Alexandrin, M.Y., Zazovskaya, E.P., Konstantinov, E.A., Shishkov, V.A., Lazukova, L.I., Chepurnaya, A.A., Kuderina, T.M., Ivanov, M.M., Kuzmenkova, N.V., Darin, A.V., Solomina, O.N., 2020. The Holocene paleoenvironmental history of Western Caucasus (Russia) reconstructed by multi-proxy analysis of the continuous sediment sequence from Lake Khuko. The Holocene 31, 368–379. https://doi.org/10.1177/0959683620972782

Grieser, J., Giommes, R., Bernardi, M., 2006. New LocClim – theLocal Climate Estimator of FAO, Geophys. Res. Abstr., 8, 08305.

Grimm, E., 1987. CONISS: a Fortran 77 Program for stratigraphically constraint cluster analysis by the 655 method of incremental squares. Computers and Geosciences 13, 13-35.

Gudbrandsson, S., Wolff-Boenisch, D., Gislason, S.R., Oelkers, E.H., 2011. An experimental study of crystalline basalt dissolution from 2⩽pH⩽11 and temperatures from 5 to 75°C. Geochimica et Cosmochimica Acta 75, 5496–5509. https://doi.org/10.1016/j.gca.2011.06.035

Guiot, J., 1990. Methodology of the last climatic cycle reconstruction in France from pollen data. Palaeogeography, Palaeoclimatology, Palaeoecology 80, 49–69.

Guiot, J., de Beaulieu, J. L., Cheddadi, R., David, F., Ponel, P., Reille, M., 1993. The climate in Western Europe during the last Glacial/Interglacial cycle derived from pollen and insect remains.Palaeo-geography, Palaeoclimatology, Palaeoecology 103, 73–93.

Günther, F., Thiele, A., Gleixner, G., Xu, B., Yao, T., Schouten, S., 2014. Distribution of bacterial and archaeal ether lipids in soils and surface sediments of Tibetan lakes: Implications for GDGT-based proxies in saline high mountain lakes. Organic Geochemistry 67, 19–30. https://doi.org/10.1016/j.orggeochem.2013.11.014

Herzschuh, U., 2007. Reliability of pollen ratios for environmental reconstructions on the Tibetan Plateau. J. Biogeography 34, 1265–1273. https://doi.org/10.1111/j.1365-2699.2006.01680.x

Hijmans, R.J., Phillips, S., Leathwick, J., Elith, J., 2020. Dismo: Species Distribution Modeling. R package version 1.3-3. https://cran.r-project.org/web/packages/dismo/

Hopmans, E.C., Schouten, S., Sinninghe Damsté, J.S., 2016. The effect of improved chromatography on GDGT-based palaeoproxies. Org. Geochem. 93, 1-6. https://doi.org/10.1016/j.orggeochem.2015.12.006

Hovsepyan, R., Willcox, G., 2008. The earliest finds of cultivated plants in Armenia: evidence from charred remains and crop processing residues in pisé from the Neolithic settlements of Aratashen and Aknashen. Vegetation History and Archaeobotany, 17(1), 63-71. https://doi.org/10.1007/s00334-008-0158-6

Hovsepyan, R. 2013. First archaeobotanical data from the basin of Lake Sevan. Archäologie in Armenien II 67, 93-10.

Hovsepyan, R. 2017. New data on archaeobotany of the Lake Sevan basin. Iran and the Caucasus 21(3), 251-276.

Huguet, C., Hopmans, E.C., Febo Ayala, W., Thompson, D.H., Sinninghe Damsté, J.S., Schouten, S., 2006. An improved method to determine the absolute abundance of glycerol dibiphytanyl glycerol tetraether lipids. Org. Geochem. 37, 1036-1041. https://doi.org/10.1016/j.orggeochem.2006.05.008

Ivy-Ochs, S., Kerschner, H., Maisch, M., Christl, M., Kubik, P.W., Schlüchter, C., 2009. Latest Pleistocene and Holocene glacier variations in the European Alps. Quat. Sci. Rev. 28, 2137–2149. https://doi.org/10.1016/j.quascirev.2009.03.009

Joannin, S., Brugiapaglia, E., de Beaulieu, J.-L., Bernardo, L., Magny, M., Peyron, O., Goring, S., Vannière, B., 2012. Pollen-based reconstruction of Holocene vegetation and climate in southern Italy: the case of Lago Trifoglietti. Clim. Past. 8, 1973–1996. https://doi.org/10.5194/cp-8-1973-2012

Joannin, S., Ali, A.A., Ollivier, V., Roiron, P., Peyron, O., Chevaux, S., Nahapetyan, S., Tozalakyan, P., Karakhanyan, A., Chataigner, C., 2014. Vegetation, fire and climate history of the Lesser Caucasus: a new Holocene record from Zarishat fen (Armenia). J. Quat. Sci. 29, 70–82. https://doi.org/10.1002/jqs.2679

Joannin, S., in prep.

Jacobson, G. L., Bradshaw, R. H., 1981. The selection of sites for paleovegetational studies. Quaternary research 16, 80-96.

Jenderedjian, K., 2005. Peatlands of Armenia, in: Steiner, G.M. (Eds.), Moore von Sibirien bis Feuerland / Mires-from Siberia to Tierra Del Fuego. Biologiezentrum/ Oberösterreichische Landesmuseen, Linz, pp. 323-333.

Jones, M.D., Abu-Jaber, N., AlShdaifat, A., Baird, D., Cook, B.I., Cuthbert, M.O., Dean, J.R., Djamali, M., Eastwood, W., Fleitmann, D., Haywood, A., Kwiecien, O., Larsen, J., Maher, L.A., Metcalfe, S.E., Parker, A., Petrie, C.A., Primmer, N., Richter, T., Roberts, N., Roe, J., Tindall, J.C., Ünal-İmer, E., Weeks, L., 2019. 20,000 years of societal vulnerability and adaptation to climate change in southwest Asia. WIREs Water 6. https://doi.org/10.1002/wat2.1330

Juggins, S., 2020. Rioja: Analysis of Quaternary Science Data. R package version 0.9-26. https://cran.r-project.org/package=rioja

Kaniewski, D., Marriner, N., Cheddadi, R., Guiot, J., Van Campo, E., 2018. The 4.2 ka BP event in the Levant. Clim. Past 14, 1529-1542. https://doi.org/10.5194/cp-14-1529-2018

Karakhanian, A., Tozalakyan, P., Grillot, J.C., Philip, H., Melkonyan, D., Paronyan, P., Arakelyan, S., 2000. Tectonic impact on the Lake Sevan environment (Armenia). Environmental geology 40(3), 279-288.

Karakhanian, A., Djrbashian, R., Trifonov, V., Philip, H., Arakelian, S., Avagian, A., 2002. Holocene-historical volcanism and active faults as natural risk factors for Armenia and adjacent countries. Journal of Volcanology and Geothermal Research 113, 319–344. https://doi.org/10.1016/S0377-0273(01)00264-5

Karakhanian, A., Arakelyan, A., Avagyan, A., & Sadoyan, T., 2017. Aspects of the seismotectonics of Armenia: New data and reanalysis. Tectonic evolution, collision, and seismicity of Southwest Asia, in: Sorkhabi, R. (Eds.), Honor of Manuel Berberian's Forty-Five Years of Research Contributions: Geological Society of America Special Paper 525, pp. 445-477.

Komárek, J., Jankovská, V., 2001. Review of the green algal genus Pediastrum: implications for pollen analytical research, J. Cramer, Berlin, Germany.

Kuhry, P., 1985. Transgressions of a raised bog across a coversand ridge originally covered with an oak-lime forest. Rev. Palaeobot. Palynol. 44, 313–353.

Lalayan, E., 1931. Mavzoleys' excavations in Soviet Armenia, Publication of Academy of Sciences of USSR, Yerevan. (In Armenian)

Lawrence, D., Philip, G., Hunt, H., Snape-Kennedy, L., Wilkinson, T.J., 2016. Correction: Long Term Population, City Size and Climate Trends in the Fertile Crescent: A First Approximation. PLoS ONE 11, e0157863. https://doi.org/10.1371/journal.pone.0157863

Lê, S., Josse, J., Husson, F., 2008. FactoMineR: An R Package for Multivariate Analysis. Journal of Statistical Software, 25(1), 1-18.

Lebreton, V., Messager, E., Marquer, L., Renault-Miskovsky, J., 2010. A neotaphonomic experiment in pollen oxidation and its implications for archaeopalynology. Review of Palaeobotany and Palynology 162, 29–38. https://doi.org/10.1016/j.revpalbo.2010.05.002

Lemcke, G., Sturm, M., 1997. δ18O and trace element measurements as proxy for the reconstruction of climate changes at Lake Van (Turkey): preliminary results, in: Dalfes, H.N., Kukla, G.,Weiss, H. (Eds.), Third Millennium BC Climate Change and Old World Collapse, NATO ASI Series 49, Springer, Berlin, pp. 653–678.

Leroy, S.A.G., Tudryn, A., Chalié, F., López-Merino, L., Gasse, F., 2013. From the Allerød to the mid-Holocene: palynological evidence from the south basin of the Caspian Sea. Quat. Sci. Rev. 78, 77–97. https://doi.org/10.1016/j.quascirev.2013.07.032

Leroyer, C., Joannin, S., Aoustin, D., Ali, A. A., Peyron, O., Ollivier, V., Tozalakyan, P., Karakhanyan, A., Fany, J., 2016. Mid Holocene vegetation reconstruction from Vanevan peat (south eastern shore of Lake Sevan, Armenia). Quaternary International, 395, 5-18. http://dx.doi.org/10.1016/j.quaint.2015.06.008

Li, Y., Xu, Q., Yang, X., Chen, H., Lu, X., 2005. Pollen-vegetation relationship and pollen preservation on the Northeastern Qinghai-Tibetan Plateau. Grana 44, 160–171. https://doi.org/10.1080/00173130500230608

Li, J., Pancost, R.D., Naafs, B.D.A., Yang, H., Zhao, C., Xie, S., 2016. Distribution of glycerol dialkyl glycerol tetraether (GDGT) lipids in a hypersaline lake system. Organic Geochemistry 99, 113–124. https://doi.org/10.1016/j.orggeochem.2016.06.007

Liaw, A., Wiener, M., 2002. Classification and regression by randomForest. R news 2, 18–22.

Lind, D., Taslakyan, L., 2005. Restoring the fallen blue sky: management issues and environmental legislation for Lake Sevan, Armenia. Environs 29, 29-103.

Lindsay, I., Smith, A.T., 2006. A History of Archaeology in the Republic of Armenia. Journal of Field Archaeology, 31(2), pp. 165-184

Loomis, S.E., Russell, J.M., Sinninghe Damsté, J.S., 2011. Distributions of branched GDGTs in soils and lake sediments from western Uganda: Implications for a lacustrine paleothermometer. Organic Geochemistry 42, 739–751. https://doi.org/10.1016/j.orggeochem.2011.06.004

Loomis, S.E., Russell, J.M., Ladd, B., Street-Perrott, F.A., Sinninghe Damsté, J.S., 2012. Calibration and application of the branched GDGT temperature proxy on East African lake sediments. Earth and Planetary Science Letters 357–358, 277–288. https://doi.org/10.1016/j.epsl.2012.09.031

Lytle, D.E., Wahl, E.R., 2005.Palaeoenvironmental reconstructions using the modern ana-logue technique: the effects of sample size and decision rules. The Holocene 15, 554–566. https://doi.org/10.1191/0959683605hl830rp

Ma, Y., Liu, K., Feng, Z., Sang, Y., Wang, W., Sun, A., 2008. A Survey of Modern Pollen and Vegetation along a South-North Transect in Mongolia. J. Biogeogr. 35, 1512–1532. https://doi.org/10.1111/j.1365-2699.2007.01871.x

Magny, M., Leuzinger, U., Bortenschlager, S., Haas, J.N., 2006. Tripartite climate reversal in Central Europe 5600–5300 years ago. Quat. res. 65, 3–19. https://doi.org/10.1016/j.yqres.2005.06.009

Martin, C., Ménot, G., Thouveny, N., Davtian, N., Andrieu-Ponel, V., Reille, M., Bard, E., 2019. Impact of human activities and vegetation changes on the tetraether sources in Lake St Front (Massif Central, France). Org. Geochem. 135, 38–52. https://doi.org/10.1016/j.orggeochem.2019.06.005

Martin, C., Ménot, G., Thouveny, N., Peyron, O., Andrieu-Ponel, V., Montade, V., Davtian, N., Reille, M., Bard, E., 2020. Early Holocene Thermal Maximum recorded by branched tetraethers and pollen in Western Europe (Massif Central, France). Quat. Sci. Rev. 228, 106109. https://doi.org/10.1016/j.quascirev.2019.106109

Martínez-Sosa, P., Tierney, J.E., Stefanescu, I.C., Dearing Crampton-Flood, E., Shuman, B.N., Routson, C., 2021. A global Bayesian temperature calibration for lacustrine brGDGTs. Geochimica et Cosmochimica Acta 305, 87–105. https://doi.org/10.1016/j.gca.2021.04.038

McGovern, P., Jalabadze, M., Batiuk, S., Callahan, M.P., Smith, K.E., Hall, G.R., Kvavadze, E., Maghradze, D., Rusishvili, N., Bouby, L., Failla, O., Cola, G., Mariani, L., Boaretto, E., Bacilieri, R., This, P., Wales, N., Lordkipanidze, D., 2017. Early Neolithic wine of Georgia in the South Caucasus. Proc Natl Acad Sci USA 114, E10309–E10318. https://doi.org/10.1073/pnas.1714728114

Meliksetian, K., Neill, I., Barfod, D.N., Milne, E.J.M., Waters, E.C., Navasardyan, G., Grigoryan, E., Olive, V., Odling, N., Karakhanian, A., 2021. Pleistocene-Holocene volcanism at the Karkar geothermal prospect, Armenia. Quaternary Geochronology, 66, 101201. https://doi.org/10.1016/j.quageo.2021.101201

Messager, E., Belmecheri, S., Von Grafenstein, U., Nomade, S., Ollivier, V., Voinchet, P., Puaud, S., Courtin-Nomade, A., Guillou, H., Mgeladze, A., Dumoulin, J.-P., Mazuy, A., Lordkipanidze, D., 2013. Late Quaternary record of the vegetation and catchment-related changes from Lake Paravani (Javakheti, South Caucasus). Quat. Sci. Rev. 77, 125–140. https://doi.org/10.1016/j.quascirev.2013.07.011

Messager, E., Nomade, S., Wilhelm, B., Joannin, S., Scao, V., Von Grafenstein, U., Martkoplishvili, I., Ollivier, V., Mgeladze, A., Dumoulin, J.-P., Mazuy, A., Belmecheri, S., Lordkipanidze, D., 2017. New pollen evidence from Nariani (Georgia) for delayed postglacial forest expansion in the South Caucasus. Quat. res. 87, 121–132. https://doi.org/10.1017/qua.2016.3

Mezhlumyan, S.K., 1972. Paleo-fauna of eneolith, bronze and iron periods in Armenia, Publication of Academy of Sciences of Armenia, Yerevan (In Russian).

Mnatsakanyan, H.H., 1952. Archaeological excavations in drained part of Lake Sevan, Publication of Academy of Sciences of Armenia, Yerevan (In Armenian).

Moore, P., Webb, J.A., Collinson, M.E., 1991. Pollen analysis, Blackwell Scientific Publications, London.

Moreno-Sanchez, R., Sayadyan, H.Y., 2005. Evaluation of the forest cover in Armenia. International Forestry Review 7, 113-127. https://doi.org/10.1505/ifor.2005.7.2.113

Mudie, P.J., Leroy, S.A.G., Marret, F., Gerasimenko, N.P., Kholeif, S.E.A., Sapelko, T., Filipova-Marinova, M., 2011. Nonpollen palynomorphs: Indicators of salinity and environmental change in the Caspian–Black Sea–Mediterranean corridor, in : Buynevich, I. , Yanko-Hombach, V., Gilbert, A.S, Martin, R.E. (Eds.), Geology and Geoarchaeology of the Black Sea Region: Beyond the Flood Hypothesis, Geological Society of America Special Paper 473, pp. 89-115.

Naafs, B.D.A., Gallego-Sala, A.V., Inglis, G.N., Pancost, R.D., 2017a. Refining the global branched glycerol dialkyl glycerol tetraether (brGDGT) soil temperature calibration. Org. Geochem. 106, 48–56. https://doi.org/10.1016/j.orggeochem.2017.01.009

Naafs, B.D.A., Inglis, G.N., Zheng, Y., Amesbury, M.J., Biester, H., Bindler, R., Blewett, J., Burrows, M.A., del Castillo Torres, D., Chambers, F.M., Cohen, A.D., Evershed, R.P., Feakins, S.J., Gałka, M., Gallego-Sala, A., Gandois, L., Gray, D.M., Hatcher, P.G., Honorio Coronado, E.N., Hughes, P.D.M., Huguet, A., Könönen, M., Laggoun-Défarge, F., Lähteenoja, O., Lamentowicz, M., Marchant, R., McClymont, E., Pontevedra-Pombal, X., Ponton, C., Pourmand, A., Rizzuti, A.M., Rochefort, L., Schellekens, J., De Vleeschouwer, F., Pancost, R.D., 2017b. Introducing global peat-specific temperature and pH calibrations based on brGDGT bacterial lipids. Geochimica et Cosmochimica Acta 208, 285–301. https://doi.org/10.1016/j.gca.2017.01.038

Ning, D., Zhang, E., Shulmeister, J., Chang, J., Sun, W., Ni, Z., 2019. Holocene mean annual air temperature (MAAT) reconstruction based on branched glycerol dialkyl glycerol tetraethers from Lake Ximenglongtan, southwestern China. Organic Geochemistry 133, 65–76. https://doi.org/10.1016/j.orggeochem.2019.05.003

Ollivier, V., Joannin, S., Roiron, P., Nahapetyan, S., Chataigner, C., 2011. Travertinization and Holocene morphogenesis in Armenia: A reading grid of rapid climatic changes impact on the landscape and societies between 9500-4000 cal. BP in the Circumcaspian regions? European Archaeologist 36, 26–31.

Ollivier V., Fontugne M., Hamon C., Decaix A., Hatté C., Jalabadze M., 2018. Neolithic water management and flooding in the Lesser Caucasus (Georgia). Quaternary Science Reviews 197, 267-287.

Ön, Z.B., Greaves, A.M., Akçer-Ön, S., Özeren, M.S., 2021. A Bayesian test for the 4.2 ka BP abrupt climatic change event in southeast Europe and southwest Asia using structural time series analysis of paleoclimate data. Climatic Change 165, 7. https://doi.org/10.1007/s10584-021-03010-6

Palmisano, A., Lawrence, D., de Gruchy, M.W., Bevan, A., Shennan, S., 2021. Holocene regional population dynamics and climatic trends in the Near East: A first comparison using archaeo-demographic proxies. Quat. Sci. Rev. 252, 106739. https://doi.org/10.1016/j.quascirev.2020.106739

Parmegiani, N., Poscolieri, M., 2003. DEM data processing for a landscape archaeology analysis (Lake Sevan-Armenia). International archives of photogrammetry remote sensing and spatial information sciences, 34, 255-258.

Pearson, E. J., Juggins, S., Talbot, H. M., Weckström, Jan., Rosén, P., Ryves, D. B., Roberts, S. J., and Schmidt, R., 2011. A lacustrine GDGT-temperature calibration from the Scandinavian Arctic to Antarctic: renewed potential for the application of GDGT-paleothermometry in lakes. Geochim. Cosmochim. Ac. 75, 6225–6238, https://doi.org/10.1016/j.gca.2011.07.042

Perşoiu, A., Ionita, M., Weiss, H., 2019. Atmospheric blocking induced by the strengthened Siberian High led to drying in west Asia during the 4.2 ka BP event – a hypothesis. Clim. Past 15, 781–793. https://doi.org/10.5194/cp-15-781-2019

Peyron, O., Magny, M., Goring, S., Joannin, S., de Beaulieu, J.-L., Brugiapaglia, E., Sadori, L., Garfi, G., Kouli, K., Ioakim, C., Combourieu-Nebout, N., 2013. Contrasting patterns of climatic changes during the Holocene across the Italian Peninsula reconstructed from pollen data. Clim. Past 9, 1233–1252. https://doi.org/10.5194/cp-9-1233-2013

Peyron, O., Combourieu-Nebout, N., Brayshaw, D., Goring, S., Andrieu-Ponel, V., Desprat, S., Fletcher, W., Gambin, B., Ioakim, C., Joannin, S., Kotthoff, U., Kouli, K., Montade, V., Pross, J., Sadori, L., Magny, M., 2017. Precipitation changes in the Mediterranean basin during the Holocene from terrestrial and marine pollen records: a model–data comparison. Clim. Past 13, 249–265. https://doi.org/10.5194/cp-13-249-2017

Prasad, A.M., Iverson, L.R. and Liaw, A., 2006. Newer classification and regression tree techniques: bagging and random forests for ecological prediction. Ecosystems 9(2), 181-199.

Prentice, I.C., 1985. Pollen representation, source area, and basin size: toward a unified theory of pollen analysis. Quaternary Research, 23(1), 76-86.

Prentice, C., Guiot, J., Huntley, B., Jolly, D., Cheddadi, R., 1996. Reconstructing biomes from palaeoecological data: a general method and its application to european pollen data at 0 and 6 ka. Climate Dynamics 12, 185–194.

Qian, H., Hongyan, L., Shilei, Y., Weihua, Y., Zhaoliang, S., 2019. Differentiated roles of mean climate and climate stability on post-glacial birch distributions in northern China. The Holocene 29, 1758–1766. https://doi.org/10.1177/0959683619862038

Ramezani, E., Marvie Mohadjer, M.R., Knapp, H.-D., Theuerkauf, M., Manthey, M., Joosten, H., 2013. Pollen–vegetation relationships in the central Caspian (Hyrcanian) forests of northern Iran. Review of Palaeobotany and Palynology 189, 38–49. https://doi.org/10.1016/j.revpalbo.2012.10.004

Reille, M., 1992-1998. Pollen et Spores d'Europe et d'Afrique du nord, Laboratoire de Botanique Historique et Palynologie, Universite d'Aix-Marseille, Marseille.

Reimer, P.J., Austin, W.E.N., Bard, E., Bayliss, A., Blackwell, P.G., Ramsey, C.B., Butzin, M., Cheng, H., Edwards, R.L., Friedrich, M., Grootes, P.M., Guilderson, T.P., Hajdas, I., Heaton, T.J., Hogg, A.G., Hughen, K.A., Kromer, B., Manning, S.W., Muscheler, R., Palmer, J.G., Pearson, C., vander Plicht, J., Reimer, R.W., Richards, D.A., Scott, E.M., Southon, J.R., Turney, C.S.M., Wacker, L., Adophi, F., Büntgen, U., Capano, M., Fahrni, S., Fogtmann-Schulz, A., Friedrich, R., Kudsk, S., Miyake, F., Olsen, J., Reinig, F., Sakamoto, M., Sookdeo, A., Talamo, S., 2020. The IntCal20Northern Hemisphere radiocarbon calibrationcurve (0–55 cal kBP). Radiocarbon 62 (4), 725–757. https://doi.org/10.1017/RDC.2020.41

Ricci, A., D'Anna, M.B., Lawrence, D., Helwing, B., Aliyev, T., 2018. Human mobility and early sedentism: the Late Neolithic landscape of southern Azerbaijan. Antiquity 92, 1445–1461. https://doi.org/10.15184/aqy.2018.230

Ritchie, K., Wouters, W., Mirtskhulava, G., Jokhadze, S., Zhvania, D., Abuladze, J., Hansen, S., 2021. Neolithic fishing in the South Caucasus as seen from Aruchlo I, Georgia. Archaeological Research in Asia 25, 100252. https://doi.org/10.1016/j.ara.2020.100252

Roberts, N., Reed, J.M., Leng, M.J., Kuzucuoğlu, C., Fontugne, M., Bertaux, J., Woldring, H., Bottema, S., Black, S., Hunt, E., Karabiyikoğlu, M., 2001. The tempo of Holocene climatic change in the eastern Mediterranean region: new high-resolution crater-lake sediment data from central Turkey. The Holocene 11, 721–736. https://doi.org/10.1191/09596830195744

Roberts, N., 2002. Did prehistoric landscape management retard the post-glacial spread of woodland in Southwest Asia? Antiquity 76, 1002–1010. https://doi.org/10.1017/S0003598X0009181X

Roberts, N., Eastwood, W.J., Kuzucuoğlu, C., Fiorentino, G., Caracuta, V., 2011. Climatic, vegetation and cultural change in the eastern Mediterranean during the mid-Holocene environmental transition. The Holocene 21, 147–162. https://doi.org/10.1177/0959683610386819

Roberts, C.N., Woodbridge, J., Palmisano, A., Bevan, A., Fyfe, R., Shennan, S., 2019. Mediterranean landscape change during the Holocene: Synthesis, comparison and regional trends in population, land cover and climate. The Holocene 29, 923–937. https://doi.org/10.1177/0959683619826697

Russell, J.M., Hopmans, E.C., Loomis, S.E., Liang, J., Sinninghe Damsté, J.S., 2018. Distributions of 5- and 6-methyl branched glycerol dialkyl glycerol tetraethers (brGDGTs) in East African lake sediment: Effects of temperature, pH, and new lacustrine paleotemperature calibrations. Organic Geochemistry 117, 56–69. https://doi.org/10.1016/j.orggeochem.2017.12.003

Ryabogina, N., Borisov, A., Idrisov, I., Bakushev, M., 2018. Holocene environmental history and populating of mountainous Dagestan (Eastern Caucasus, Russia). Quaternary International 516, 111–126. https://doi.org/10.1016/j.quaint.2018.06.020

Sagona, A., Kiguradze, T., 2003. On the origins of the Kura-Araxes cultural complex. Archaeology, in: Smith, T., Rubinson, K.S. (Eds.), Archaeology in the borderlands: investigations in Caucasia and beyond. Cotsen Institute of Archaeology, Los Angeles, pp. 38-94

Sagona, A., 2017. The Archaeology of the Caucasus: from Earliest Settlements to the Iron Age. Cambridge University Press, Cambridge.

St Jacques, J.M., Cumming, B.F., Sauchyn, D.J., Smol, J.P., 2015. The bias and signal attenuation present in conventional pollen-based climate reconstructions as assessedby early climate data from Minnesota, USA. PLoS One 10, 1–17. https://doi.org/10.1371/journal.pone.0113806

Salonen, J.S., Verster, A.J., Engels, S., Soininen, J., Trachsel, M., Luoto, M., 2016. Calibrating aquatic microfossil proxies with regression-tree ensembles: Cross-validation with modern chironomid and diatom data. The Holocene 26, 1040–1048. https://doi.org/10.1177/0959683616632881

Salonen, J.S., Korpela, M., Williams, J.W., Luoto, M., 2019. Machine-learning based reconstructions of primary and secondary climate variables from North American and European fossil pollen data. Scientific reports 9, 1–13.

Sayadyan, Y.V., Aleshinskaya, Z.V., Khanzadyan, E.V., 1977. Late glacial deposits and archaeology of the Sevan Lake, in: Sayadyan, Y.V. (Eds.), Geology of the Quaternary Period (Pleistocene), Akad. Nauk Arm. SSR, Yerevan, pp. 91-109 (in Russian).

Sayadyan, Y.V., 1978. Postglacial Times in Armenia and Adjacent Regions, vol. XII. Studia Geomorphologica Carpatho-Balcanica, Krakow, pp. 77-93.

Sayadyan, Y.V., 1983. Men and environment in postglacial period in Lake Sevan basin and neighbourhood areas. In: Problems of Quaternary Geology in Armenia. Yerevan, pp 67-73 (In Russian).

Sayadyan, Y.V., 2009. The Newest Geological History of Armenia. Gitutun publish, Nat. Acad. Sciences, Yerevan (In Russian).

Sayadyan, H.Y., 2011. Valuation of mountain forests: case study Armenia. Annals of agrarian science. Republic of Georgia, 9(1), 144-148.

Schouten, S., van der Meer, M. T., Hopmans, E. C., Rijpstra, W. I. C., Reysenbach, A.-L., Ward, D. M., Sinninghe Damsté, J.S., 2007. Archaeal and bacterial glycerol dialkyl glycerol tetraether lipids in hot springs of Yellowstone National Park. Applied and Environmental Microbiology 73(19), 6181–6191.

Shanahan, T.M., Hughen, K.A., Van Mooy, B.A.S., 2013. Temperature sensitivity of branched and isoprenoid GDGTs in Arctic lakes, Org. Geochem. 64, 119–128. https://doi.org/10.1016/j.orggeochem.2013.09.010

Sharifi, A., Pourmand, A., Canuel, E.A., Ferer-Tyler, E., Peterson, L.C., Aichner, B., Feakins, S.J., Daryaee, T., Djamali, M., Beni, A.N., Lahijani, H.A.K., Swart, P.K., 2015. Abrupt climate variability since the last deglaciation based on a high-resolution, multi-proxy peat record from NW Iran: The hand that rocked the Cradle of Civilization? Quat. Sci. Rev. 123, 215–230. https://doi.org/10.1016/j.quascirev.2015.07.006

Shumilovskikh, L.S., Tarasov, P., Arz, H.W., Fleitmann, D., Marret, F., Nowaczyk, N., Plessen, B., Schlütz, F., Behling, H., 2012. Vegetation and environmental dynamics in the southern Black Sea region since 18kyr BP derived from the marine core 22-GC3. Palaeogeography, Palaeoclimatology, Palaeoecology 337–338, 177–193. https://doi.org/10.1016/j.palaeo.2012.04.015

Sinninghe Damsté, J.S., Rijpstra, W.I.C., Foesel, B.U., Huber, K.J., Overmann, J., Nakagawa, S., Kim, J.J., Dunfield, P.F., Dedysh, S.N., Villanueva, L., 2018. An overview of the occurrence of ether- and ester-linked iso-diabolic acid membrane lipids in microbial cultures of the Acidobacteria: Implications for brGDGT paleoproxies for temperature and pH. Organic Geochemistry 124, 63–76. https://doi.org/10.1016/j.orggeochem.2018.07.006

Smith, A.T., 2015. The Political Machine: Assembling Sovereignty in the Bronze Age Caucasus. Princeton University Press, Princeton.

Solomina, O.N., Bradley, R.S., Hodgson, D.A., Ivy-Ochs, S., Jomelli, V., Mackintosh, A.N., Nesje, A., Owen, L.A., Wanner, H., Wiles, G.C., Young, N.E., 2015. Holocene glacier fluctuations. Quat. Sci. Rev. 111, 9–34. https://doi.org/10.1016/j.quascirev.2014.11.018

Solomon, J.C., Shulkina, T.V., Schatz, G.E., 2014. Red List of the Endemic Plants of the Caucasus: Armenia, Azerbaijan, Georgia, Iran, Russia, and Turkey, Missouri Botanical Garden Press, Saint Louis.

Sosson, M., Rolland, Y., Müller, C., Danelian, T., Melkonyan, R., Kekelia, S., Adamia, S., Babazadeh, V., Kangarli, T., Avagyan, A., Galoyan, G., Mosar, J., 2010. Subductions, obduction and collision in the Lesser Caucasus (Armenia, Azerbaijan, Georgia), new insights, in: Sosson, M., Kaymakci, N., Stephenson, R., Bergerat, F., Starostenko, V. (Eds.), Sedimentary Basin Tectonics from the Black Sea and Caucasus to the Arabian Platform, Geological Society of London, Special Publication 340, pp. 329-352. https://doi.org/10.1144/SP340.14

St Jacques, J.M., Cumming, B.F., Sauchyn, D.J., Smol, J.P., 2015. The bias and signal attenuation present in conventional pollen-based climate reconstructions as assessed by early climate data from Minnesota, USA. PLoS One 10, 1-17. https://doi.org/10.1371/journal.pone.0113806.

Stanyukovich, K. V., 1973. Vegetation of the Mountains of the USSR. The Tadjik Academy of Sciences Presse, Dushanbe (in Russian).

Stevens, L.R., Wright, H.E., Ito, E., 2001. Proposed changes in seasonality of climate during the Lateglacial and Holocene at Lake Zeribar, Iran. The Holocene 11, 747–755. https://doi.org/10.1191/09596830195762

Stevens, L.R., Ito, E., Schwalb, A., Wright, H.E., 2006. Timing of Atmospheric Precipitation in the Zagros Mountains Inferred from a Multi-Proxy Record from Lake Mirabad, Iran. Quat. res. 66, 494–500. https://doi.org/10.1016/j.yqres.2006.06.008

Stockhecke, M., Bechtel, A., Peterse, F., Guillemot, T., Schubert, C.J., 2021. Temperature, precipitation, and vegetation changes in the Eastern Mediterranean over the last deglaciation and Dansgaard-Oeschger events. Palaeogeography, Palaeoclimatology, Palaeoecology 577, 110535. https://doi.org/10.1016/j.palaeo.2021.110535

Sun, Q., Chu, G.Q., Liu, M.M., Xie, M.M., Li, S.Q., Ling, Y., Wang, X.H., Shi, L.M., Jia, G.D., Lü, H.Y., 2011. Distributions and temperature dependence of branched glycerol dialkyl glycerol tetraethers in recent lacustrine sediments from China and Nepal. J. Geophys. Res. 116, G01008. https://doi.org/10.1029/2010jg001365

Takhtajyan, A.L., 1941. Botanical-geographic overview of Armenia. Work Papers of Institute of Botany of Armenian Academy of Sciences/Branch of USSR Academy of Sciences 2, 180 (in Russian).

Telford, R.J., Birks, H.J.B., 2005. The secret assumption of transfer functions: problems with spatial autocorrelation in evaluating model performance. Quat. Sci. Rev. 24, 2173–2179. https://doi.org/10.1016/j.quascirev.2005.05.001

Telford, R.J., Birks, H.J.B., 2009. Evaluation of transfer functions in spatially structured environments. Quat. Sci. Rev. 28, 1309–1316. https://doi.org/10.1016/j.quascirev.2008.12.020

Telford, R.J., Birks, H.J.B., 2011. QSR Correspondence "is spatial autocorrelation introducing biases in the apparent accuracy of palaeoclimatic reconstructions?". Quat. Sci. Rev. 30, 3210–3213. https://doi.org/10.1016/j.quascirev.2011.07.019

Ter Braak, C.J.F., Van Dam, H., 1989. Inferring pH from diatoms: A comparison of old and new calibration methods. Hydrobiologia 178, 209–223.

Ter Braak, C.J.F., Juggins, S., Birks, H.J.B., Van der Voet, H., 1993. Weighted averaging partial least squares regression (WA-PLS): definition and comparison with other methods for species-environment calibration, chap. 25, Elsevier Science Publishers, Amsterdam, pp. 525–560.

Tumanyan, M.R., 1971. On the history of lake Sevan basin vegetation in holocene. Academy of Sciences of Armenian SSR, Biological Journal, T.XXIV 11, 57-61 (in Russian).

Tumajanov, I.I., Tumanyan, M.R., 1973. New data on the history of forest vegetation in Masrik plain in Holocene. Academy of Sciences of Armenian SSR, Biological Journal, T.XXVI 12, 24-28 (in Russian).

Turner, R., Roberts, N., Jones, M.D., 2008. Climatic pacing of Mediterranean fire histories from lake sedimentary microcharcoal. Global and Planetary Change 63, 317–324. https://doi.org/10.1016/j.gloplacha.2008.07.002

Turner, R., Roberts, N., Eastwood, W.J., Jenkins, E., Rosen, A., 2010. Fire, climate and the origins of agriculture: micro-charcoal records of biomass burning during the last glacial-interglacial transition in Southwest Asia. J. Quaternary Sci. 25, 371–386. https://doi.org/10.1002/jqs.1332

Van Geel, B., van der Hammen, T., 1978. Zygnemataceae in Quaternary Colombian sediments. Rev. Palaeobot. Palynol. 25, 377–392.

Van Geel, B., Coope, G.R, van der Hammen, T., 1989. Palaeoecology and stratigraphy of the Lateglacial type section at Usselo (The Netherlands). Rev. Palaeobot. Palynol. 60, 25–129.

Van Geel, B., Grenfell, H.R., 1996. Spores of Zygnemataceae, in: Jansonius, J., McGregor D.C. (Eds.) Palynology: principles and applications, Am. Ass. Strat. Palynol. Found.,Vol. 1, pp. 173–179.

Van Geel, B., 2002. Non-Pollen Palynomorphs, in: Smol, J.P., Birks, H.J.B., Last, W.M., Bradley, R.S., Alverson, K. (Eds.), Tracking Environmental Change Using Lake Sediments. Developments in Paleoenvironmental Research. Springer, Dordrecht, pp. 99–119. https://doi.org/10.1007/0-306-47668-1_6

Van Geel, B., Heijnis, H., Charman, D.J., Thompson, G., Engels, S., 2014. Bog burst in the eastern Netherlands triggered by the 2.8 kyr BP climate event. The Holocene 24, 1465–1477. https://doi.org/10.1177/0959683614544066

Van Zeist, W., Woldring, H., Stapert, D., 1975. Late Quaternary vegetation and climate of southwestern Turkey. Palaeohistoria 17, 53–143.

Volodicheva, N., 2002. The Caucasus, in: Shahgedanova, M. (Eds.), The Physical Geography of Northern Eurasia. Oxford University Press, New York, pp. 350-376.

Wang, H. Y., Liu, W. G., Zhang, C. L., Wang, Z., Wang, J. X., Liu, Z. H., Dong, H. L., 2012. Distribution of glycerol dialkyl glycerol tetraethers in surface sediments of Lake Qinghai and surrounding soil, Org. Geochem. 47, 78–87. https://doi.org/10.1016/j.orggeochem.2012.03.008

Watson, B.I., Williams, J.W., Russell, J.M., Jackson, S.T., Shane, L., Lowell, T.V., 2018. Temperature variations in the southern Great Lakes during the last deglaciation: Comparison between pollen and GDGT proxies. Quaternary Science Reviews 182, 78–92. https://doi.org/10.1016/j.quascirev.2017.12.011

Weber, Y., Sinninghe Damsté, J.S., Zopfi, J., De Jonge, C., Gilli, A., Schubert, C.J., Lepori, F., Lehmann, M.F., Niemann, H., 2018. Redox-dependent niche differentiation provides evidence for multiple bacterial sources of glycerol tetraether lipids in lakes. Proc. Natl. Acad. Sci. USA 115, 10926–10931. https://doi.org/10.1073/pnas.1805186115

Wei, H., Zhao, Y., 2015. Surface pollen and its relationships with modern vegetation and climate in the Tianshan Mountains, northwestern China. Veget. Hist. Archaeobot. 25, 19–27. https://doi.org/10.1007/s00334-015-0530-2

Weijers, J.W., Schouten, S., Linden, M., Geel, B., Sinninghe Damsté, J.S., 2004. Water table related variations in the abundance of intact archaeal membrane lipids in a Swedish peat bog. FEMS Microbiology Letters 239, 51–56.

Weijers, J.W., Schouten, S., Hopmans, E.C., Geenevasen, J.A., David, O.R., Coleman, J.M., Pancost, R.D., Sinninghe Damsté, J.S., 2006. Membrane lipids of mesophilic anaerobic bacteria thriving in peats have typical archaeal traits. Environmental Microbiology 8(4), 648–657. https://doi.org/10.1111/j.1462-2920.2005.00941.x

Weijers, J.W., Schouten, S., van den Donker, J.C., Hopmans, E.C., Sinninghe Damsté, J.S., 2007. Environmental controls on bacterial tetraether membrane lipid distribution in soils. Geochem. Cosmochim. Acta 71, 703–713. https://doi.org/10.1016/j.gca.2006.10.003

Weiss, H., Courty, M.-A., Wetterstrom, W., Guichard, F., Senior, L., Meadow, R., Curnow, A., 1993. The genesis and collapse of third millennium north Mesopotamian civilization. Science 261, 995–1004.

Weiss, H., 2016. Global megadrought, societal collapse and resilience at 4.2–3.9 ka BP across the Mediterranean and west Asia. Magazine 24, 62–63. https://doi.org/10.22498/pages.24.2.62

Wick, L., Lemcke, G., Sturm, M., 2003. Evidence of Lateglacial and Holocene climatic change and human impact in eastern Anatolia: high-resolution pollen, charcoal, isotopic and geochemical records from the laminated sediments of Lake Van, Turkey. The Holocene 13, 665–675. https://doi.org/10.1191/0959683603hl653rp

Wright, H.E., Ammann, B., Stefanova, I., Atanassova, J., Margalitadze, N., Wick, L., Blyakharchuk, T., 2003. Late-glacial and Early-Holocene Dry Climates from the Balkan Peninsula to Southern Siberia, in: Tonkov, S. (Eds.), Aspects of Palynology and Palaeoecology – Festschrift in Honour of Elissaveta Bozilova. Pensoft Publishers, Sofia, pp. 127-136. https://doi.org/10.1016/j.quascirev.2009.02.001

Wu, W., Zheng, H., Hou, M., Ge, Q., 2018. The 5.5 cal ka BP climate event, population growth, circumscription and the emergence of the earliest complex societies in China. Sci. China Earth Sci. 61, 134–148. https://doi.org/10.1007/s11430-017-9157-1

Wünnemann, B., Demske, D., Tarasov, P., Kotlia, B.S., Reinhardt, C., Bloemendal, J., Diekmann, B., Hartmann, K., Krois, J., Riedel, F., Arya, N., 2010. Hydrological evolution during the last 15kyr in the Tso Kar lake basin (Ladakh, India), derived from geomorphological, sedimentological and palynological records. Quat. Sci. Rev. 29, 1138-1155. https://doi.org/10.1016/j.quascirev.2010.02.017

Xiao, W., Wang, Y., Zhou, S., Hu, L., Yang, H., Xu, Y., 2016. Ubiquitous production of branched glycerol dialkyl glycerol tetraethers (brGDGTs) in global marine environments: a new source indicator for brGDGTs. Biogeosciences 13, 5883–5894. https://doi.org/10.5194/bg-13-5883-2016.

Xu, Q.H., Li, Y.C., Zhou, L.P., Li, Y.Y., Zhang, Z.Q., Lin, F.Y., 2007. Pollen flux and vertical dispersion in coniferous and deciduous broadleaved mixed forest in the Changbai Mountains. Chinese Science Bulletin 52 (11), 1540–1544.

Xu, Q., Li, Y., Tian, F., Cao, X., Yang, X., 2009. Pollen assemblages of tauber traps and surface soil samples in steppe areas of China and their relationships with vegetation and climate. Review of Palaeobotany and Palynology 153, 86–101. https://doi.org/10.1016/j.revpalbo.2008.07.003

Xu, Q., Cao, X., Tian, F., Zhang, S., Li, Y., Li, M., Li, J., Liu, Y., Liang, J., 2014. Relative pollen productivities of typical steppe species in northern China and their potential in past vegetation reconstruction. Sci. China Earth Sci. 57, 1254–1266. https://doi.org/10.1007/s11430-013-4738-7

Yang, H., Pancost, R.D., Dang, X., Zhou, X., Evershed, R.P., Xiao, G., Tang, C., Gao, L., Guo, Z., Xie, S., 2014. Correlations between microbial tetraether lipids and environmental variables in Chinese soils: Optimizing the paleo-reconstructions in semi-arid and arid regions. Geochimica et Cosmochimica Acta 126, 49–69. https://doi.org/10.1016/j.gca.2013.10.041

Yu, X., Zhou, W., Franzen, L.G., Xian, F., Cheng, P., Jull, A.J.T., 2006. High-resolution peat records for Holocene monsoon history in the eastern Tibetan Plateau. Sci. China 49, 615–621. https://doi.org/10.1007/s11430-006-0615-y

Zanchetta, G., Bar-Matthews, M., Drysdale, R.N., Lionello, P., Ayalon, A., Hellstrom, J.C., Isola, I., Regattieri, E., 2014. Coeval dry events in the central and eastern Mediterranean basin at 5.2 and 5.6ka recorded in Corchia (Italy) and Soreq caves (Israel) speleothems. Global and Planetary Change 122, 130–139. https://doi.org/10.1016/j.gloplacha.2014.07.013

Zanchetta, G., Regattieri, E., Isola, I., Drysdale, R. N., Bini, M., Baneschi, I., and Hellstrom, J. C., 2016. The so-called "4.2 event" in the central Mediterranean and its climatic teleconnections, Alp. Med. Quat. 29, 5–17.

Zhao, Y., Herzschuh, U., 2009. Modern pollen representation of source vegetation in the Qaidam Basin and surrounding mountains, north-eastern Tibetan Plateau. Veget. Hist. Archaeobot. 18, 245–260. https://doi.org/10.1007/s00334-008-0201-7

Zhao, Y., Yu, Z., Chen, F., 2009. Spatial and temporal patterns of Holocene vegetation and climate changes in arid and semi-arid China. Quaternary International 194, 6–18. https://doi.org/10.1016/j.quaint.2007.12.002

Zhang, Y.-J., Duo, L., Pang, Y.-Z., Felde, V.A., Birks, H.H., Birks, H.J.B., 2018. Modern pollen assemblages and their relationships to vegetation and climate in the Lhasa Valley, Tibetan Plateau, China. Quaternary International 467, 210–221. https://doi.org/10.1016/j.quaint.2018.01.040

Zheng, Z., Huang, K., Xu, Q., Lu, H., Cheddadi, R., Luo, Y., Beaudouin, C., Luo, C., Zheng, Y., Li, C., Wei, J., Du, C., 2008. Comparison of climatic threshold of geographical distribution between dominant plants and surface pollen in China. Sci. China Ser. D-Earth Sci. 51, 1107–1120. https://doi.org/10.1007/s11430-008-0080-x

Zielhofer, C., Fletcher, W.J., Mischke, S., De Batist, M., Campbell, J.F.E., Joannin, S., Tjallingii, R., El Hamouti, N., Junginger, A., Stele, A., Bussmann, J., Schneider, B., Lauer, T., Spitzer, K., Strupler, M., Brachert, T., Mikdad, A., 2017. Atlantic forcing of Western Mediterranean winter rain minima during the last 12,000 years, Quat. Sci. Rev. 157, 29–51, 2017. http://dx.doi.org/10.1016/j.quascirev.2016.11.037

Zink, K.-G., Vandergoes, M.J., Bauersachs, T., Newnham, R.M., Rees, A.B.H., Schwark, L., 2016. A refined paleotemperature calibration for New Zealand limnic environments using differentiation of branched glycerol dialkyl glycerol tetraether (brGDGT) sources. Journal of Quaternary Science 31, 823–835. https://doi.org/10.1002/jqs.2908